We appreciate the constructive comments on our manuscript provided by the referees. We have taken these into consideration and modified the paper in response. Overall, the suggestions have made this a stronger paper. The responses are explained in our response to reviewer comments below with all of our responses are in red type. Changes or additions to the manuscript are *red and italic*. At the end of the responses (pg 9) the complete manuscript is provided with all changes marked since the initial submission.

Overall: This paper reports very useful observations and contains a lot of useful analysis. However, certain portions of the discussion (principally in Section 4, but also 1 paragraph in Section 3) are poorly supported at best. The conclusions drawn by those sections may well be correct, but the manuscript (MS) does not demonstrate them. My hope is that the authors can rewrite the portions of the MS that are not adequately supported and address some other issues I catalog below so that the MS can be published in ACP.

Furthermore, the paper reports that oil and gas (OG) VOC contributes to about 20 ppbv of O3 in Rocky Mountain (ROMO). This is very hard to reconcile with the modeling results of McDuffie (2016), which are reporting that at BAO, peak ozone concentrations would only be 3 ppbv lower if OG VOC were not present. This paper is cited in the MS, but this critical difference is not mentioned. It does not seem likely that both of these results can be correct: OG VOC only adds about 3 ppbv at BAO but 20 ppbv at ROMO. If there is an explanation for this, or if there is some other explanation for this discrepancy, it should be discussed. If the authors are not aware of an explanation for the discrepancy, that should be acknowledged.

It is stated in the paper that we are investigating the influence of O&G emissions for specific, well characterized upslope events. Our approach and focus differs substantially from the McDuffie et al. work. Their study reports average O&G contributions, and they use VOC abundances from 2012 with NO$_x$ and O$_3$ measurements from 2014. This paper is highly reliant on a set of model experiments. Co-authors on this paper, are also co-authors on the McDuffie paper. We are not criticizing the approach in McDuffie et al, but rather acknowledging the limitation of the approach and the strength in approaching this problem using multiple approaches. Since the McDuffie et al., work, there have been many other ozone-focused papers. Most relevant, Cheadle et al. [2017] estimate that on individual days, oil and gas O3 precursors can contribute up to 30 ppbv of ozone. The reviewer mentions this paper later and points out that this 30 ppbv is associated with both VOC and NOx precursors. Also relevant is Zaragoza et al. [2017]. This paper shows that on days with large ozone production, anthropogenic VOCs dominate the photochemistry. The PAN ratios on these days indicate that alkane chemistry is important.

A close examination of Figures 3, 12, 1S and 2S shows that impacts during upslope events can be quite pronounced, while O&G impacts averaged over the whole summer season are significantly lower. Therefore, we use an *event based approach* focused on upslope events from the NFRMA to show that Front Range emissions, in particular O&G coupled with urban emissions, are driving the ozone exceedances in ROMO. We have added text to the manuscript to clarify this difference. In addition, we have also de-emphasized the 20 ppb increase in O$_3$ at ROMO is just from oil and gas due to the uncertainty in the calculations associated with the method we have used. In particular we have added that other species like OVOCs may be contributing to this increase in O$_3$. However, this is conservative because many of the OVOCs (MEK, acetone and acetaldehyde) can be produced from alkane oxidation.

Cheadle LC, Oltmans SJ, Petron G, Schnell RC, Mattson EJ, Herndon SC, et al.. **Surface ozone in the Colorado northern Front Range and the influence of oil and gas development during FRAPPE/DISCOVER-AQ in summer 2014**. Elem Sci Anth. 2017;5:61. DOI: http://doi.org/10.1525/elementa.254

Zaragoza, J., Callahan, S., McDuffie, E. E., Kirkland, J., Brophy, P., Durrett, L., et al. (2017). **Observations of acyl peroxy nitrates during the Front Range Air Pollution and Photochemistry Éxperiment (FRAPPÉ).** Journal of Geophysical Research: Atmospheres, 122. https://doi.org/10.1002/2017JD027337

5

Section 4.2 First, the PAN & PPN discussion in the 3rd paragraph is difficult to follow, seems tendentious, and it's not clear to me that it adds to the analysis. PPN was not measured at ROMO, but the arguments here seem to rely analysis in a paper by Lindaas (submitted) that says that high PPN/PAN ratios indicate substantial contribution to PAN and PPN from OG alkanes. If these arguments are important to the overall analysis, they should be clarified and simplified. It appears to me that the key result is simply that previous work studying the front range has demonstrated that OG alkanes are a key precursor to PAN and PPN in this area; the measurements of PAN and ROMO don't seem to add much to this.

We have clarified and simplified this discussion to focus on what the presence of PAN indicates at ROMO (PAN likely formed from OG alkanes).

15

Page 12-13 – analysis based on alkyl nitrates. These two paragraphs, which lead to a key finding of the MS (20 ppbv O3 from OG VOC) are at best inadequately supported. The logic of many of the steps in this analysis is not transparent: simply put, I can't see why its true. These paragraphs are also very, very sparse on citations, so more support is certainly needed.
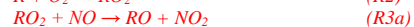The following has been added to the manuscript, which highlights the point that a limited number of similar types of analysis are reported in the literature.

As noted in Rosen et al. (2004), only a limited number of studies report the correlation of O_3 or O_x with alkyl nitrates, with half of the studies using the sum of alkyl nitrates ($\sum$ANs) because a non-selective technique was used that did not allow for individual speciation of the alkyl nitrates (Flocke et al., 1991; Neuman et al., 2012; O'Brien et al., 1995; Perring et al., 2013; Roberts et al., 1996; Rosen et al., 2004). Flocke et al. (1991) reported the correlation of $\square C_2$–C_5 straight chain alkane-derived nitrates plus a single C_4 branched chain alkane-derived nitrate with O_x measured at Shauinsland, Germany.

P12 lines 11-14. I'm afraid I am not familiar with using alkyl nitrate formation as a proxy for O3 production in this way. Please provide citations to papers that explain the logic of this approach, or do so here (ie with Chemical Equations, etc).
The following text has been added to better illustrate the utility of using alkyl nitrates as a proxy for ozone production:

Because the production of O_3 and alkyl nitrates is tied to their common precursor, the alkyl peroxy radical (RO_2), correlation between O_3 and the C_2-C_5 alkyl nitrates is expected. As a first step, the y-intercept is used to estimate the background O_3 value for the event period prior to the start of the upslope event. As shown in Table 3, each of the individual alkyl nitrates gives a slightly different background O_3 value (y-intercept); however, they are all within a few ppbv of each other, providing a reasonable estimate of the background O_3 during that time period. The values reported for this work are also in the range of values reported by McDuffie et al. (2016) for BAO during summer 2014. The main source of the C_2-C_5 alkyl nitrates is the photochemical production from their parent alkane precursors, as outlined in the following simplified reaction scheme:

$$RH + OH \rightarrow R + H_2O \qquad (R1)$$
$$R + O_2 \rightarrow RO_2 \qquad (R2)$$
$$RO_2 + NO \rightarrow RO + NO_2 \qquad (R3a)$$
$$RO_2 + NO + M \rightarrow RONO_2 + M \qquad (R3b)$$
$$NO_2 + h\upsilon \rightarrow NO + O \qquad (R4)$$
$$O + O_2 + M \rightarrow O_3 + M \qquad (R5)$$

As shown by Reactions 1-5, alkyl nitrates share a common photochemical production mechanism with O_3. However, O_3 formation results from the photolysis of NO_2 (R4) whereas the formation of alkyl nitrates serve as a sink for NO_x, RO and RO_2, which affects O_3 production efficiency (Atkinson et al., 1982; Ranschaert et al., 2000; Russo et al., 2010b). Nonetheless, based on these reactions, it is expected that under a wide range of conditions O_3 and alkyl nitrates should be correlated as they are

produced concurrently in the atmosphere (e.g. Abeleira et al., 2018; Day et al., 2003; Flocke et al., 1991; Perring et al., 2013; Rosen et al., 2004; Russo et al., 2010b).

Lines 14-16 "For the August 8 and 18 events, the overall air mass composition (Figure 11) and photochemical age (Figure 12)
5   indicate that the source region emissions and processing times in the Front Range were comparable and these assumptions are valid." The assumptions are the three stated on lines 11-14. First, Figs 11 and 12 don't tell us anything about co-location of NOx and VOC. Second, Fig 11 does not allow us to compare anything about Aug 8 and 18, because the data for those two days is averaged on Fig 11. Fig 12 does show that the photochemical ages appear to be quite similar for the high ozone hours (Fig 12 is hourly data?) on 8/8 and 8/18, and on the order of 15 hours. But that is not direct support for any of the three
10 assumptions. In short, this paragraph does not help me understand why this approach makes sense if the 3 assumptions are valid, nor why the data shown in Figs 11 and 12 supports the validity of those 3 assumption.

The wrong figure was cited – it should have been Figure 14 (now Figure 12). This has been corrected. Additionally, the following text has been added to detail that these assumptions were met:

15   *Analogous to PAN, alkyl nitrates are photochemically produced simultaneously with ozone in the atmosphere. Here, we use coincident observations of alkyl nitrates during these elevated O_3 periods to estimate the contribution of the light alkanes from oil and gas emissions to O_3 production. Alkyl nitrate formation can be used as a proxy for O_3 production if we make the following assumptions. First, their photochemical production is rapid compared to removal processes and mixing across gradients. The rate of alkyl nitrate formation is tied to*
20 *its parent alkane's concentration and reaction rate with the hydroxyl radical (OH), which is the hydroxyl radical reactivity (R1), as this is the rate limiting step in alkyl peroxy radical (RO_2) formation. In NFRMA areas that are influenced by oil and gas emissions, the hydroxyl radical reactivity values for the alkyl nitrate parent alkanes are high (Figure 11), resulting in rapid production compared to their removal rates. Because of their relatively long lifetimes ($\sim \leq 10$ days for summer), the C_2-C_5 alkyl nitrates can be transported long distances and serve as a*
25 *temporary reservoir for NO_x, ultimately leading to O_3 production in downwind or remote regions (e.g., Clemitshaw et al., 1997; Flocke et al., 1998; Roberts et al., 1998). For the upslope events on August 8 and 18, the assumption that photochemical production of the alkyl nitrates is rapid compared to removal processes is supported based on the rates of formation (hours) versus their removal (days). Second, the precursor compounds (VOCs and NO_x) both have sources in Weld County, where significant oil and gas development exists NO_x was elevated during both*
30 *events (not shown) and the 2014 National Emissions Inventory (US EPA, 2017) suggests Weld County has the largest emissions of NO_x and VOCs in the state, and so it is reasonable to assume that emissions are collocated. The collocation of sources indicates these air masses likely contained sufficient NO_x for alkyl nitrate and O_3 formation and the excess O_3 is clearly related to VOC and NO_x emissions from the oil and gas region. There could be NO_x additions to the air mass as it moves west, but this does not violate the assumption because of the timescale*
35 *for the transport, which is relatively fast. Third, transport time from the source region (NFRMA) to the park is rapid (on the order of hours). This assumption is validated by the time series plots shown in Figure 13, where during the upslope events, rapid increases in mixing ratios are observed within an hour of when the wind shifts to an upslope direction.*

          In general, this approach is similar to estimating O_3 production efficiency and background O_3 using O_x/NO_z
40 *but instead we use the individual alkyl nitrates in NO_z because of the abundance of alkanes emitted from oil and gas operations. Moreover, we can better apportion the photochemical processing from the source region emissions because we are using an ensemble of individual compounds that have known rate constants, branching ratios and processing times, as opposed to using a bulk parameter such as a NO_z, where the composition is not accurately known. For the oil and gas influenced upslope events at ROMO, PAN, O_3, NO_x, and alkyl nitrates all show*
45 *coincident increases (Figure 3; Benedict et al., 2018). For the August 8 and 18 events, the overall air mass composition (Figures 3, 12, 1S and 2S) and photochemical age (Figure 13) indicate that the source region emissions and processing times in the Front Range were comparable and these assumptions are valid.*

3

Page 13 lines 3 – 8. Again, this simple correlation of alkyl nitrates to O3 as a way of attributing O3 to alkenes doesn't seem obvious to me, and the MS just does not explain why this is logical. The agreement in results when this is done for various alkyl nitrates is interesting, but not convincing, since this analysis does not tell us anything about the contribution from other VOC (non-alkanes) that are simultaneously contributing to O3.

In short, this analysis needs to be justified.

We have addressed these concerns in the previous responses by including more detail describing how the excess ozone was calculated from the $O_3/RONO_2$ plots.

Page 13 lines 8-9 – consistency with Cheadle 2017. **Be careful here.** First, Cheadle is claiming that on the day when Cheadle suggests the highest contribution of OG emissions to measured O3 (8/13), NOx was also attributable to OG. Therefore, Cheadle is attributing up to 30 ppb O3 to all OG emissions, not just OG VOC. Second, the conditions on the high O3 days were light winds. In these conditions, emissions can
accumulate to very high levels in air over Weld Cty (where Cheadle measured). For example
on 8/3 Platteville flasks measured 50 – 150 ppb ethane – far higher than ethane at ROMO on 8/8 or 8/18. Therefore, I don't agree that Cheadle's results are really consistent with what the MS is claiming about O3 at ROMO attributable to OG VOC.

We agree that different weather conditions existed for the determination Cheadle et al. made compared with those we are making. The stagnation conditions experienced on the day Cheadle et al. used to make their estimate of OG emissions to O_3 are often the conditions that lead to elevated O_3 in ROMO if the elevated concentrations of VOCs, NO_x, and O_3 are transported to ROMO from the Front Range. The air masses that we measured during upslope events originated on the Front Range, and the mix of VOCs suggest air masses highly influenced by O&G with elevated O_3. It is also worth noting that the methods for determining the increase in O_3 from O&G are quite different. We have added the following clarification to the text that regarding NOx.

Second, the precursor compounds (VOCs and NO_x) both have sources in Weld County, where significant oil and gas development exists NO_x was elevated during both events (not shown) and the 2014 National Emissions Inventory (US EPA, 2017) suggests Weld County has the largest emissions of NO_x and VOCs in the state, and so it is reasonable to assume that emissions are collocated. The collocation of sources indicates these air masses likely contained sufficient NO_x for alkyl nitrate and O_3 formation and the excess O_3 is clearly related to VOC and NO_x emissions from the oil and gas region.

Page 13 line 16 – again, Fig 11 simply does not show how similar airmasses were on Aug 8 and 18 because the data for those two days is avgd. in the figure. There is no question, based on the results shown in the MS, that OG contributes to O3 at ROMO. However, the analysis used in the MS to estimate that 20 ppbv of the peak O3 on these two days is attributable to OG VOC seems very questionable.

Figure 14 (now Figure 12) should be referenced here instead of Figure 11. This was overlooked when the order of figures was rearranged before submission. We have also added a reference to Figure 3 which shows that the mix of species is similar on both days. Regarding the estimate of 20 ppb O3, we have expanded our attribution to include other VOCs (i.e. OVOCs) and noted the elevated NOx present. We have also added that this is an upper limit of the oil and gas contribution to elevated O3 on these days.

These values represent an upper limit on the excess O_3 produced from NFRMA air masses transported to ROMO that were dominated by oil and gas emissions. Other compounds produced photochemically in situ (e.g., PAN and acetone) provide similar values to the alkyl nitrates for the attributed O_3 (not shown). The alkyl nitrate correlation method does not allow us to

4

explicitly separate the impact of NOₓ, additional OVOCs or other species such as alkenes (Figure 11), which all likely contribute to ozone production.

5 **Section 3** Page 8-9, paragraph beginning on p 8 line 19, and Figure 6 This paragraph makes a number of unsupported statements – which may very well be true – and is poorly organized. Figure 6 does not well support the statements and has issues itself. As it stands now, the statements that NMHC levels at ROMO "can be comparable . . . to other [sic] urban/industrial areas" and "Observed mixing ratios during afternoons with
upslope flow can be similar to those observed simultaneously in the Front Range" are
10 not supported. These statements appear to be the main point of the paragraph, but they are not supported
by Fig 6, since Fig 6 clearly shows significantly lower MRs for ROMO than everywhere else. I suspect that this has a lot to do with the averaging, so I don't doubt the statements above, but again, the statements are not supported.
We have reorganized this paragraph to better convey the main point – that peak values observed at ROMO are at the levels observed in other areas. We readily acknowledge that the majority of observed values at ROMO are
15 lower. We have added citations supporting lower mixing ratios at remote sites (Jobson et al., 1994; Rindsland et al., 2002; Rudolph, 1995; Simpson et al., 2012). We have clarified this in the text with the following:

At their peak values, NMHC mixing ratios observed at ROMO can be of comparable magnitude to urban/industrial regions, further suggesting a significant impact of the polluted NFRMA on ROMO during specific events. The range of mixing ratios
20 *observed at ROMO overlaps the range of observations compiled by Baker et al. (2008) from 28 cities across the United States.*

- First and foremost with the figure, what data are being compared. I presume that the transect whole air samples are all collected during the day (I don't think this is stated either way), while the ROMO data are averages / medians for 24-hour
25 data? Since Fig 3 appears to show that at ROMO the spikes in NMHC are all daytime only when upslope is happening, comparing the 24 ROMO average to daytime-only (?) transect
data arguably artificially decreases the ROMO data in this sense.
We have added the following sentence to explain the high transect mixing ratios in the transect samples compared to ROMO:
30
The transect samples were collected next to the road and only during daytime hours, when upslope flow from the east is prevalent.

- Then, the figure compares these values to PAO data and BAO data. But, those are probably 24hour averages (???) and may
35 well include high values measured at night with low boundary layers (?). I'm speculating, but there is no discussion of any of this. How comparable are these values? The simple way to handle this might be to compare values at ROMO during upslope events to values at PAO, or during afternoons at ROMO. But right now, the statements are not supported.
Most of the data presented are from datasets that cover 24 hours of measurements. The exceptions to this are the transect samples and the Baker et al. data which represent a range of observations from 28 different cities. We
40 have added the time of data collection for each study to the caption in Figure 6 to clarify the comparison across sites.

There are other issues with the paragraph and figure that need to be addressed.
45 - BAO is first introduced here, but the acronym is not defined, and no context about the site (ie, "a site in the NFRMA somewhat more removed from OG production than PAO") is provided.
We have added a description of BAO.

5

- The fact that ethyne and benzene are similar at ROMO and during the transects, and they are far more similar to PAO and BAO levels than the alkanes, needs some discussion. It's just mentioned in passing. ???

The mixing ratios of benzene and ethyne likely reflect background values. These species have longer atmospheric lifetimes and are relatively well mixed unless measurements are made in a plume. We have added some discussion of these values likely representing background to the manuscript.

The ROMO and transect ethyne mixing ratios presented in this figure likely represent background as there is significant overlap for all sites with the range of means from 28 U.S. cities. Benzene mixing ratios also suggest background values for the ROMO and transect samples while slightly elevated mixing ratios at BAO and PAO indicate additional sources, likely from oil and gas (Halliday et al., 2016).

- For the figure:
o Define the limits of the boxes and whiskers for the data from this study
o Define the error bars for the Baker 2008 data
o Ideally, draw vertical lines or something like that between each set of symbols (that is, a line between the ethane and propane symbols, a line btwn the propane and i-C4 symbols, a line btwn i- and n-C4 symbols, etc.) As it is now it's really hard to read the graph.

We have made the suggested changes.

Minor Issues
- It's really helpful for future readers if you put the dates of the observations (months and the year) in the abstract
We have added the months and year of measurement to the abstract.

- P4 line 6 – what time of day were the canisters collected?
We have added that the canister samples were generally collected between 13:00-18:00.

- P4, lines 14-16 – this is not very clear or helpful. First, I think it means that the analytical system was calibrated for multiple species with a whole air standard which was run every 10 samples. Second, the precisions listed are very good (1%!) . . . but at what mole fraction? Comparable to the mole fractions measured at ROMO? A specific reference here is needed, even it it is one of the 3 papers listed in the pvs sentence.

We have added the following information to the manuscript to clarify the range of standards analyzed:

The whole air working standards employed for this work have mixing ratios representative of clean free tropospheric air (NMHCs mixing ratios on the order of ~10-100 pptv) and suburban air (NMHC mixing ratios on the order of ~1-2 ppbv), thus bracketing the low and high ranges for the measurements at ROMO (e.g. Russo et al., 2010a).

- P6, lines 16-19. This passage about the contents of propane LPG cylinders is poorly drafted and mildly inaccurate (it appears to carry over an error from Wikipedia about the specifics of the hd-5 standard). The "mild error:" HD-5 must be >90% propane, <5% propene, and <2.5% C4+, according to astm 1835 (those are liquid vol %s). There is no limit of ethane except the 10% upper limit (since the gas must be 90% propane).
This passage needs proper references.

We have updated this section with the correct information and have added the following reference: ASTM Standard D1835-16, 2016, "Standard Specification for Liquefied Petroleum (LP) Gases," ASTM International, West Conshohocken, PA, 2016, DOI: 10.1520/ D1835-16, www.astm.org.

- Page 7 – top – headings. Having two headings here is superfluous... I suggest you replace the two headings with "3. Temporal and Spatial Trends in Volatile Organic Compounds"
We agree and we have made the change as suggested.

6

- Page 7, line 17-18 – significant MeOH from oil and gas has been observed in Utah by NOAA. Is this not the case in the DJ in the summertime? I can believe it since I think it's main use for OG is inhibition of hydrate formation in cold weather. But I think that would be valuable to note; it should not be assumed that OG is not part of the source mix for MeOH at ROMO.

We have added this possibility to the text. The text now reads:

Methanol has vegetative sources and potential oil and gas sources in some basins where it is used during cold weather to inhibit equipment freezing (Warneke et al., 2014), but, more importantly for the Front Range, in summer this trace gas also comes from animal agriculture and confined animal feeding operations (CAFOs)(Sun et al., 2008). Given the co-location of agricultural and oil and gas related sources in NE Colorado, it is difficult to ascertain the magnitude of each source, but it is likely that agriculture and CAFOS would be the larger source in the NFRMA and surrounding areas during the summer.

- Page 7 lines 19-20. It won't be obvious to some readers what "hourly 2-day ensemble back trajectories" are. (I don't know in what sense they are "ensembles"). How about "two-day back trajectories were calculated for each hour of the study"

We have clarified this. It now reads: *To better understand VOC influence from these sources, air mass transport patterns were examined with back trajectories started hourly at 10 m above ground with previous air mass positions traced backward in time for two days using the Hybrid Single-Particle Lagrangian Integrated Trajectory (HYSPLIT) model ver 4.9.*

- Figure 4. The units are not clear. Is this the % of trajectories that include (go through) each pixel, or that end in each pixel? Clarify. The term ORT seems to imply the former to this reader, but the units at the top of the color bar says "% ends." Also the units are cut off on the figure. %ends / g???

We have added the following information to the caption to clarify the units. "*Units are the percent of total endpoints in each grid cell. Endpoints are upwind air mass locations calculated every hour for two days back in time for every trajectory that arrived at the receptor during the duration of the study period.*"

Reviewer 2:

General Comments:

This manuscript contributes a valuable documentation to ozone and VOC data for the Rocky Mountain National Park (ROMO) during the FRAPPE campaign time period of summer 2014. I recommend that it be published in ACP.

-I agree with some of the concerns of the first reviewer - plus the following.

For future search/reference to this data, please add a date reference such as "summer 2014" to the abstract.

We have added the months and year of measurement to the abstract.

I recommend that the paper recognizes the main FRAPPE "infrastructure" funding sources ie NCAR and the Colorado Department of Public Health and Environment (CDPHE), as well as NASA - if only for archive maintainance.

We have added recognition of the FRAPPE team and funding sources to the acknowledgements section.

Figure 1 Maybe there could be a more contextual discussion of ozone for the FRAPPE campaign time period compared to the full time series shown in this figure?

We have added several sentences to address the levels of O_3 during the study compared to the record. To the introduction we have added:

In general, O_3 mixing ratios were lower during the summer of 2014 than in the preceding four years; specifically, the peak O_3 mixing ratios were lower and there were fewer hours when mixing ratios exceeded 70 ppb. Weather conditions, including greater rainfall and cloud cover than is typical during the summer months, contributed to lower O_3 levels in ROMO and on the Front Range (Cheadle et al., 2017; McDuffie et al., 2016).

Figure 6 Maybe add PAN?

Because PAN data are not available for most of the other sites and studies included in the figure, we did not add PAN to Figure 6.

10

Volatile Organic Compounds and Ozone in Rocky Mountain National Park during FRAPPÉ

Katherine B. Benedict[1], Yong Zhou[1], Barkley C Sive[2], Anthony J. Prenni[2], Kristi A. Gebhart[3], Emily V. Fischer[1], Ashley Evanoski-Cole[1], Amy P. Sullivan[1], Sara Callahan[1], Bret A. Schichtel[3], Huiting Mao[4], Ying Zhou[4], Jeffrey L. Collett, Jr. [1]

[1]Department of Atmospheric Science, Colorado State University, Fort Collins, CO 80523, USA
[2]National Park Service, Air Resources Division, Lakewood, CO 80225, USA
[3]National Park Service, Air Resources Division, Fort Collins, CO 80523, USA
[4]Department of Chemistry, State University of New York College of Environmental Science and Forestry, Syracuse, NY, 13210, USA

Correspondence to: Katherine B. Benedict (katherine.benedict@colostate.edu)

Abstract. The 2014 Front Range Air Pollution and Photochemistry Éxperiment (FRAPPÉ) aimed to better characterize summertime air quality in the Northern Front Range Metropolitan Area (NFRMA) and its impact on surrounding areas. As part of this study, measurements of gas and particle phase species were collected in Rocky Mountain National Park (ROMO), located in the mountains west of the urban North Front Range corridor from July – October 2014. We report on measurements of ozone from two locations in the park and a suite of volatile organic compounds (VOCs) measured using a continuous real-time gas chromatography system and a quadrupole proton-transfer reaction-mass spectrometer at the ROMO Longs Peak air quality site. We also measured VOCs using canister samples collected along transects connecting the NFRMA and ROMO. These datasets show that ROMO is impacted by NFRMA emission sources, and high observed mixing ratios of VOCs associated with oil and gas extraction (e.g. ethane) and urban sources (e.g. ethene and C_2Cl_4) occur during periods of upslope transport. Hourly ozone mixing ratios exceeded 70 ppb during six events. Two of the six events were largely associated with VOCs from the oil and gas sector, three high ozone events were associated with a mixture of VOCs from urban and oil and gas sources, and one high ozone event was driven by a stratospheric intrusion. For the high ozone events most associated with emissions from oil and gas activities, we estimate that VOCs and NO_x from sources along the Front Range contributed ~20 ppbv of additional ozone.

1. Introduction

Ozone (O_3) is a regulated pollutant that can impact both human and ecosystem health. Monthly mean daytime O_3 has been increasing in the Rocky Mountains and throughout much of the west (Strode et al., 2015), and there are concerns about O_3 levels and exceedances of the O_3 National Ambient Air Quality Standard (NAAQS) at high elevation sites (Christensen et

al., 2015; Musselman and Korfmacher, 2014). In Rocky Mountain National Park (ROMO), a protected Class I area with millions of visitors each year (National Park Service, 2017), O_3 mixing ratios often exceed the current NAAQS standard of 70 ppb and vegetation injury thresholds (Kohut et al., 2012). A timeline of O_3 mixing ratios measured at the ROMO Longs Peak (ROMO-LP) CASTNET (Clean Air Status and Trends NETwork) site from January 2010 to December 2015 is shown in Figure

5   1. In general, O_3 mixing ratios were lower during the summer of 2014 than in the preceding four years; specifically, the peak O_3 mixing ratios were lower and there were fewer hours when mixing ratios exceeded 70 ppb. Weather conditions, including greater rainfall and cloud cover than is typical during the summer months, contributed to lower O_3 levels in ROMO and on the Front Range (Cheadle et al., 2017; McDuffie et al., 2016). In addition to transport and O_3 production from regional source emissions, the U.S. Intermountain West (all elevations) has a higher probability of stratospheric O_3 reaching the troposphere

10   from tropopause folding (related to mid-latitude jet or cutoff low) and stratospheric intrusion events (Lin et al., 2015; Musselman and Korfmacher, 2014; Reddy and Pfister, 2016; Wooldridge et al., 1997). At Great Basin National Park, another high elevation park in the west, elevated O_3 mixing ratios have been shown to be impacted by long-range transport, regional transport, and high-altitude transport (Christensen et al., 2015), highlighting the complex nature of O_3 sources at these Intermountain West sites.

15   ROMO is in close proximity to the North Front Range Metropolitan Area (NFRMA), which includes Denver, Boulder, and Fort Collins (urban areas) (Figure 2), in addition to the Denver-Julesburg Basin, which has seen significant increases in oil and natural gas production. For example, in nearby Weld County, the number of active wells doubled between January 2008 and July 2015, to over 27,000 [Colorado Oil and Gas Conservation Commission (COGCC) 2/2016]. Previous studies have extensively characterized NFRMA volatile organic compound (VOC) emissions, including those from oil and

20   natural gas extraction activities, and their influence on air quality at the Boulder Atmospheric Observatory (Gilman et al., 2013; McDuffie et al., 2016; Pétron et al., 2012; Swarthout et al., 2013). These studies demonstrate the extremely high mixing ratios of alkanes in the NFRMA, with maximum observed ethane and propane mixing ratios exceeding 100 ppbv (Swarthout et al., 2013) compared to mean values of 0.56-8.74 ppbv and 0.29-6.05 ppbv, respectively, in urban areas (Baker et al., 2008). The extent that these emissions reach ROMO has not been previously determined, although previous studies have shown that

10

agricultural ammonia emissions from a similar geographic source region are frequently transported into ROMO (Beem et al., 2010; Benedict et al., 2013).

The Front Range Air Pollution and Photochemistry Experiment (FRAPPÉ) took place in the summer of 2014 and was focused on characterizing summertime air quality and O_3 formation in the NFRMA. FRAPPÉ included extensive ground, mobile and aircraft measurements throughout the region, including ROMO. This work focuses on a primary goal of the measurements at ROMO – to better understand the factors contributing to high O_3 in the park including potential contributions of the NFRMA. These data are meant to inform strategies to reduce O_3 in the park and the exposure of visitors and ecosystems to elevated O_3 levels. Measurements at the ROMO Longs Peak site (40.2783°N, 105.5457°W; 2784 m ASL) during FRAPPÉ included a suite of VOCs in addition to O_3 and meteorological parameters, which are routinely measured at the site. Whole air canister samples were also collected along U.S. Route 34 from the NFRMA to higher elevation sites (3600 m) to examine spatial variations in VOC concentrations (Figure 2). Ozone and meteorological measurements were also made at an additional high elevation site within ROMO, located off Trail Ridge Road (ROMO-TR; 40.3900° N, 105.6865° W, 3498 m ASL). Additional measurements carried out at ROMO during FRAPPÉ are the focus of separate publications (Benedict et al., 2018; Zaragoza et al., 2017).

2. Methods

2.1 In situ Volatile Organic Compound Measurements

A cryogen-free concentration system coupled with two gas chromatographs (GC) was installed in the Colorado State University Mobile Laboratory for near real-time (1-hr sample frequency) analysis of VOCs at the Longs Peak Monitoring Station at ROMO from 17 July to 4 September 2014. Ambient air was drawn from 5.25 m above ground level using a 3 m × 0.635 cm outer diameter (o.d.) stainless steel line followed by a 3 m × 0.4 cm inner diameter (i.d.) PFA Teflon line. Air flow was maintained continuously at ~7 L min^{-1} using a metal bellows pump (MB-158, Senior Flexionics, Sharon, MA) and delivered a pressure of 10 psig. The inlet residence time was <1 s. A sub-stream of the pressurized air (~2.5 L min^{-1}) was directed to a water management system, which reduced water vapour before entering the analytical system. The water management system consisted of a 7.5 m × 0.635 cm o.d. stainless steel coil and a stainless steel liquid water reservoir, which

11

was housed in a commercial refrigerator and set at ~2° C. The total volume of the system was ~380 ml, yielding a residence time of <10 s. The VOC analytical system was similar to those used in previous studies (Abeleira et al., 2017; Sive et al., 2005) and utilized a Qdrive 2s102K cryocooler (Chart, Inc., Troy, NY) that was capable of cooling a sample enrichment loop from 100 °C to -180 °C in 25 minutes for sample concentration. Additional details are provided in the supplemental information.

5 Two different whole air standards were alternately analysed every 10 samples throughout the campaign for quantification of the target gases as well as to monitor the system's performance; the standard mixing ratios were representative of clean and polluted levels encountered at ROMO. The measurement precision, represented by the relative standard deviation (RSD) of the peak areas for each compound in the standards, was 1-8% for the non-methane hydrocarbons (NMHCs), 3-11% for halocarbons, and 3-5% for alkyl nitrates. A list of VOCs measured during this study using the *in situ* GC is shown in Table 1.

10 **2.2.1 Canister sampling**

Whole air canister samples were collected at eight non-urban locations during the campaign to investigate the spatial distributions of VOCs. Canister samples were collected in the Big Thompson Canyon along Route 34 en route to the ROMO Longs Peak site three days a week during the campaign; several transects were also continued up Trail Ridge Road to the continental divide at the Alpine Visitors Center in ROMO (ROMO-TR, Figure 2) when upslope transported was expected.

15 Canisters were typically collected between 13:00 – 18:00 (local time). A total of 39 individual VOCs were quantified from the canister samples in our laboratory at Colorado State University using a five-channel, three-GC analytical system, which employed three FIDs, one ECD and one mass spectrometer (MS). The gases analysed included C_2-C_{10} NMHCs, C_1-C_2 halocarbons, C_1-C_5 alkyl nitrates, selected reduced sulphur compounds and OVOCs (oxygenated VOCs). A complete list of VOCs measured from the canister samples using the lab analytical system is included in Table 1.

20 The analytical system and methodology used for this study are similar to those used in previous studies (Russo et al., 2010b; Sive, 1998; Zhou et al., 2010). Multiple standards were used during sample analysis (analysed every 10 samples). The whole air working standards employed for this work have mixing ratios representative of clean free tropospheric air (NMHCs mixing ratios on the order of ~10-100 pptv) and suburban air (NMHC mixing ratios on the order of ~1-2 ppbv), thus bracketing the low and high ranges for the measurements at ROMO (e.g. Russo et al., 2010a). The measurement precision, represented

12

by the relative standard deviation (RSD) of the peak areas for each compound in the whole air standards, was 1-8% for the NMHCs, 3-10% for halocarbons, and 3-5% for the alkyl nitrates.

2.2.2 Proton Transfer Reaction-Mass Spectrometer (PTR-MS)

Selected VOCs and OVOCs were monitored in real-time by a quadrupole proton-transfer reaction-mass spectrometer located in the NPS air quality monitoring shelter (PTR-MS; Ionicon Analytik, Innsbruck, Austria) from 14 July to 8 September 2014. The PTR-MS sampled air that was continuously drawn through a 13 m $\times$ 1.27 cm o.d. (0.9525 cm i.d.) PFA Teflon inlet from 10 m above ground level. The flow rate through the sample line was ~70 L min^{-1}, resulting in a <1 s residence time. A diaphragm pump was used to draw a sub-stream of air off the main inlet line through a 1 m $\times$ 0.635 cm PFA Teflon line at a flow rate of 1 L min^{-1} from which the PTR-MS sampled.

The PTR-MS was operated with a drift tube pressure and temperature of 2.0 mbar and 45 °C, respectively, and a potential of 600 V applied over the length (9.6 cm) of the drift tube. The ion source water flow rate was 11 ml min^{-1} and the discharge current was 8 mA. A series of 30 masses was monitored continuously; six masses were monitored for diagnostic purposes while the remaining 24 masses corresponded to VOCs of interest. The dwell time for each of these 24 masses ranged from 1-10 s, yielding a total measurement cycle of ~3 min. The system was zeroed every 25 hours for 10 cycles by diverting the flow of ambient air through a heated catalytic converter (0.5% Pd on alumina at 550 °C) to determine system background signals. Calibrations for the PTR-MS system were conducted using three different high-pressure cylinders containing synthetic blends of selected NMHCs and OVOCs at ppbv levels. Each of the cylinders used in the calibrations had an absolute accuracy of <±5% for all gases. Standards were diluted to atmospheric mixing ratios (ppbv to pptv levels) with catalytic converter-prepared zero air adjusted to maintain the humidity of the sampled air for 6-10 cycles every 25-75 hours. Mixing ratios for each gas were calculated by using the normalized counts per second which were obtained by subtracting out the non-zero background signal for each compound. The PTR-MS precision was estimated from counting statistics and ranged from 6-15%.

13

2.3 Ozone measurement at Longs Peak and Trail Ridge Road

2.3.1 Trail Ridge Road

The third generation of a custom built portable O_3 monitoring system (POMS3, Air Resource Specialists, Inc., Fort Collins, CO) was deployed at a high elevation site located off of the Ute Trail in ROMO (40.3900° N, 105.6865° W, 3498 m ASL) during FRAPPÉ for O_3 and meteorological measurements. Measurements were conducted from 11 July – 18 September 2014. The system incorporated two 2B Technologies O_3 analysers, a 6.1 m sampling mast, a data acquisition system, and meteorological instruments for measurements of wind speed, wind direction, temperature, relative humidity, solar radiation, and precipitation. The POMS3 unit was fitted with solar panels and batteries sufficient for operation during the campaign. Hourly averages of O_3 and meteorological parameters were reported for this site. More information on the Trail Ridge O_3 measurements and calibration procedures can be found in the supplement.

2.3.2 Longs Peak

Ozone and meteorological measurements have been measured continuously at the ROMO Longs Peak site since 1987, as part of the National Park Service Gaseous Pollutant Monitoring Program. As a regulatory O_3 monitoring station, the sampling methods for gaseous and meteorological monitoring are based on the 40 CFR Part 58 requirements. The Longs Peak site includes a temperature-controlled shelter that houses the O_3 analyser and calibration system. The O_3 inlet and meteorological measurements are located on top of a 10-m tower. Ozone is measured by UV absorption utilizing a Thermo 49i O_3 analyzer coupled with a Thermo 49i O_3 reference station for nightly zero, precision and span checks. One minute O_3 data are recorded and hourly averages are generated from the 1-minute O_3 data. The suite of meteorological measurements include wind speed, wind direction, relative humidity, temperature, solar radiation and precipitation, and 1-minute meteorological data were acquired during FRAPPÉ. As with the POMS3 site, further details can be found in the Gaseous Pollutant Monitoring Program 2015 Quality Assurance Project Plan (https://ard-request.air-resource.com/Project/documents.aspx).

14

2.4 Data filtering to remove local source effects

Initial analysis of FRAPPÉ data showed unexpectedly high propane concentrations relative to other VOCs at the ROMO-LP site. The highest propane concentrations were associated with the lowest wind speeds, suggesting that a leaking propane tank used by a nearby youth camp (<200 m) was a local source. Typically in the U.S., propane fuel is primarily composed of propane (at least 90%), with no more than 2.5% butanes and maximum 5% propylene (ASTM Standard D1835-16, 2016). ~~Typically in the U.S., propane fuel is primarily propane (at least 90%), with the composition balance mostly containing ethane, propene, butane, and odorants. This is the HD-5 standard, Heavy Duty 5% maximum allowable propene content, and no more than 5% butanes and ethane defined by the American Society for Testing and Materials by Standard 1835 for internal combustion engines.~~

To better understand the influence of regional VOC emissions and transport on the distributions of VOCs and O_3 in ROMO, it was necessary to filter out alkane, alkene, and BTEX (benzene, toluene, ethylbenzene, xylene) data that were affected by the local emissions. In this study, data with ethane/propane ratios <1 were considered to be propane tank influenced and were removed. The resulting ratio of ethane to propane for filtered data (1.2) was similar to that determined for transect samples (1.13) taken at multiple locations in ROMO at different times, supporting the data-filtering approach.

3. Temporal and Spatial Trends in

~~3.1~~ Volatile Organic Compounds

Throughout the campaign, hourly VOC mixing ratios varied by 1 to 3 orders of magnitude (Table 1). Figure 3 and Figure S1 show this variability for several VOCs as well as for O_3 at the ROMO-LP and ROMO-TR sites from 17 July - 4 September, 2014. The C_2-C_5 alkanes, C_2-C_4 alkenes, ethyne, aromatics (benzene and toluene), C_2-C_5 alkyl nitrates, tetrachloroethylene (C_2Cl_4), trichloroethylene (C_2HCl_3) and OVOCs, such as methanol, generally had similar temporal variations during most of the study period. The similar temporal patterns suggest that many of the concentration changes are driven by meteorology, with westerly flow generally transporting cleaner air, and easterly flow transporting pollutants from the NFRMA. However, in some cases, differences between species' mixing ratio enhancements likely reflect specific sources influencing air masses that reach the park.

15

All of the VOCs from Figure 3 have sources in the NFRMA. For example, light alkanes (e.g. ethane) have oil and natural gas sources in northeastern Colorado and have been observed in high abundance along the Front Range (Abeleira et al., 2017; Gilman et al., 2013; Swarthout et al., 2013). Vehicle combustion, prevalent throughout the NFRMA, is an important source of light alkenes, ethyne, and aromatics (e.g. benzene) (Koppmann, 2007), although oil and gas emissions have also

5   been shown to be the most important source of aromatics, specifically benzene, at certain locations (Abeleira et al., 2017; Halliday et al., 2016). C_2Cl_4 and C_2HCl_3 are widely used as solvents and dry cleaning fluids and are frequently used as tracers of urban air masses (Blake et al., 1996). Methanol has vegetative sources and potential oil and gas sources in some basins where it is used during cold weather to inhibit equipment freezing (Warneke et al., 2014), but, more importantly for the Front Range, in summer this trace gas also comes from animal agriculture and confined animal feeding operations (CAFOs)(Sun et

10   al., 2008). Given the co-location of agricultural and oil and gas related sources in NE Colorado, it is difficult to ascertain the magnitude of each source, but it is likely that agriculture and CAFOs would be the larger source in the NFRMA and surrounding areas during the summer.

To better understand VOC influence from these sources, air mass transport patterns were examined with back trajectories started hourly at 10 m above ground with previous air mass positions traced backward in time for two days using

15   the Hybrid Single-Particle Lagrangian Integrated Trajectory (HYSPLIT) model ver 4.9 (Stein et al., 2015). Input data are from the North American Model with a grid resolution of 12 km (NAM12) (Janjic, 2003). Back trajectory residence time analyses are a long-established method to examine upwind air mass transport pathways for periods of interest (Ashbaugh et al., 1985). Previous back trajectory analyses for ROMO captured most meso-synoptic scale patterns, but may underestimate the easterly upslope flow into the park (Gebhart et al., 2011, 2014). In Figure 4a, the Overall Residence Time (ORT) shows the relative

20   probability for transport from the areas upwind of ROMO-LP during all hours of the study without regard to observed air mass composition. Results indicate that during the study period, air masses arrived from all directions, but areas most frequently upwind were areas to the southwest and the Front Range. Similarly, High Mixing Ratio Residence Times (HRT) were generated using only hours when a measured VOC mixing ratio at ROMO-LP exceeded the 90th percentile of study values. The HRT for ethane, which primarily is from leakage during the production and transport of natural gas (Tzompa-Sosa et al.,

25   2017), is shown in Figure 4b. A sparser pattern results from including only 10% of the hours. Many of the same areas are

16

upwind as in the ORT, but areas to the east have a higher probability of being upwind during this subset of high concentration time periods.

Figure 5 presents differences between transport patterns during high mixing ratio measurements (exceeding the 90th percentile), as compared to all study conditions. The difference maps in Figure 5 are calculated by subtracting the overall probability of transport (ORT) from the probability of transport on a high mixing ratio hour (HRT), or HRT-ORT (Poirot et al., 2001) . Figure 5a shows the results for ethane (Figure 4b – Figure 4a). This more clearly shows that high concentrations of ethane are preferentially associated with transport from northeastern Colorado, where large oil and gas emissions occur (Figure 2). Figure 5b shows a similar analysis, but for C_2Cl_4 (urban tracer) measurements. The results again point to the NFRMA, but with more of an influence from further south toward Denver because of its widespread usage in the region. Figure 5c shows results for isoprene. In this case, wooded mountainous areas to the west are upwind more often than average. Plots for ethene (tracer for fuel combustion) (Figure 5d) and ethyne (not shown) also point to the NFRMA. These results are not surprising, as upslope conditions from the east are expected to transport pollutants to the park. However, this is the first time that *in situ* VOC tracers have been used to demonstrate the many Front Range sources that impact ROMO.

At their peak values, NMHC mixing ratios observed at ROMO can be of comparable magnitude to urban/industrial regions, further suggesting a significant impact of the polluted NFRMA on ROMO during specific events. The range of mixing ratios observed at ROMO overlaps the range of observations compiled by Baker et al. (2008) from 28 cities across the United States. Although measurements at ROMO were lower than at most other locations shown in Figure 6, mixing ratios of these VOCs are much higher at ROMO than is typical for remote sites (Jobson et al., 1994; Rindsland et al., 2002; Rudolph, 1995; Simpson et al., 2012). Observed mixing ratios during afternoons with upslope flow can be similar to those observed simultaneously in the Front Range (see maximum values in Table 1). ROMO is a Class I area that is afforded the highest level of air quality protection, while these other locations are in major source regions. The fact that maximum NMHC levels at ROMO are of similar magnitude to these other areas suggests a significant impact on the park from anthropogenic emissions, at least during episodic transport. Figure 6 also includes measurements made during FRAPPÉ at the Platteville Atmospheric Observatory (PAO), a rural location surrounded by agriculture and intensive oil and gas development in northeastern Colorado (Halliday et al., 2016). Observed mixing ratios at this site tended to be the highest of those included in this figure. With the

Commented [B1]: This paragraph was reorganized.

17

exception of benzene and ethyne, measured mixing ratios from the transect samples (gray) and other measurements made in the Front Range (Abeleira et al., 2017; McDuffie et al., 2016; Swarthout et al., 2013) generally exceed those measured in ROMO. The transect samples were collected next to the road and only during daytime hours, when upslope flow from the east is prevalent. Both factors likely contribute to the larger values measured compared to the measurements at ROMO. The ROMO and transect ethyne mixing ratios presented in this figure likely represent background as there is significant overlap for all sites with the range of means from 28 U.S. cities. Benzene mixing ratios also suggest background values for the ROMO and transect samples while slightly elevated mixing ratios at BAO and PAO indicate additional sources, likely from oil and gas (Halliday et al., 2016).

The ratio of i-pentane to n-pentane has been used to identify air masses impacted by oil and gas emissions. Although this ratio varies by basin, a ratio less than one is generally indicative of oil and gas emissions (COGCC, 2007; Gilman et al., 2013; Prenni et al., 2016; Swarthout et al., 2013, 2015). During FRAPPÉ, Halliday et al. (2016) reported an i- to n-pentane ratio of 0.89 at PAO. This ratio is expected to be enhanced in areas where fuel evaporation is an important source of NMHCs (Harley et al., 1992; McGaughey et al., 2004), as i-pentane is an abundant component of gasoline and is elevated relative to n-pentane. As such, ratios in urban areas are often in the range of 1.5-4 (Baker et al., 2008; McLaren et al., 1996; Parrish et al., 1998; Russo et al., 2010a). For ROMO-LP hourly samples, shown in Figure 7, the average ratio of i-pentane to n-pentane was 1.10 throughout the campaign. The transect samples had an average ratio of 1.19 (not shown), which is 8% higher than the ROMO hourly samples. The slightly higher values along the transects ~~likely~~ may reflect impacts from nearby vehicle emissions. In Figure 7, markers are coloured by ethane mixing ratio. As seen in Figure 7, a strong oil and gas signature is evident on many sample days, with low i- to n-pentane ratios associated with higher ethane mixing ratios; similarly, higher ratios were usually associated with lower ethane mixing ratios from clean air masses transported from the west.

Figure 8 shows the spatial and temporal variability of i- to n-pentane in all of the canister transect samples, with the points sized by ethane mixing ratio (other ~~species~~ gases are shown in the supplement Figure S3). The transect samples show a general east-west gradient with lower ratios typically observed at the easternmost sites, consistent with the oil and gas production activity in this area. However, significant variability was observed throughout the study at most of the transect sampling locations, with the range encompassing conditions indicative of dominant oil and gas influence (<1), to conditions

18

more indicative of urban influences (1.93). On three occasions samples were collected from the Front Range up to the ROMO-TR site near the continental divide. Even limiting measurements to these three sampling dates at high elevation, the i- to n-pentane ratios indicated a range of air mass source histories impacted the park.

5 ~~NMHC levels observed at ROMO can be of a comparable magnitude to other urban/industrial regions, further suggesting a significant impact of the polluted NFRMA on the park. The observed mixing ratios of light NMHCs from this study are compared to those reported at other locations in Figure 6. With the exception of benzene and ethyne, measured mixing ratios from the transect samples (gray) and other measurements made in the Front Range (Abeleira et al., 2017; McDuffie et al., 2016; Swarthout et al., 2013) generally exceed those measured in ROMO. Figure 6 includes measurements made during FRAPPÉ at the Platteville Atmospheric Observatory (PAO), a rural location surrounded by agriculture and oil~~
10 ~~and gas development (Halliday et al., 2016). Except for ethyne, observed abundances of VOCs at PAO are consistently higher than observed at BAO. Observed abundances of VOCs both at ROMO and during the transect samples are more similar to average mixing ratios of VOCs measured in of 28 U.S. cities (Baker et al., 2008). Although measurements at ROMO were lower than most of the other locations shown in Figure 6, mixing ratios of these VOCs are much higher at ROMO than typical remote sites. Observed mixing ratios during afternoons with upslope flow can be similar to those observed simultaneously in~~
15 ~~the Front Range. ROMO is a Class I area that is afforded the highest level of air quality protection, while these other locations are in major source regions. The fact that NMHC levels at ROMO are of similar magnitude to these other areas suggests a significant impact on the park from anthropogenic emissions, particularly from episodic transport.~~

4. Ozone

4.1 Ozone Distributions at ROMO during FRAPPÉ

20 Ozone measurements at the ROMO-LP and ROMO-TR sites show coincident peaks for most of the FRAPPÉ study period (Figure 3), although O_3 mixing ratios were slightly higher and had considerably less variability at the ROMO-TR site. For ease of comparison, the frequency distributions of the O_3 mixing ratios are shown in Figure 9. The mean O_3 mixing ratios at ROMO-TR and ROMO-LP were 53 ppb (1-hr max: 82 ppb) and 43 ppb (1-hr max: 79 ppb), respectively, where ROMO-LP is lower in elevation and closer to the Front Range. Differences in these distributions can be attributed to several factors. First,

the Longs Peak site is located in a valley, where pollutants can be trapped by stable nocturnal inversions, allowing efficient dry deposition or the titration of O_3 by NO, as seen by the regular night time decreases in O_3 in Figure 3. In comparison, the Trail Ridge Road site near the Continental Divide, sits above the nocturnal inversion and is isolated from surface loss processes. This results in a skewed distribution toward lower mixing ratios at the Longs Peak site, with the median, 25th and 75th percentile values of 45 ppb, 36 ppb and 51 ppb, compared to the normal distribution at Trail Ridge Road with higher median, 25th and 75th percentile values of 53 ppb, 49 ppb and 57 ppb (Figure 9). Second, additional photochemical processing can occur during transport to the more distant Trail Ridge site during upslope events, resulting in slightly higher O_3 levels, as indicated by the 1-hr maximum values (ROMO-TR = 82 ppb; ROMO-LP = 79 ppb). Nevertheless, the relationship of the timelines of the O_3 data from both sites during elevated concentrations suggests they are often impacted by similar air masses (r^2=0.33, p<0.0001).

Elevated O_3 mixing ratios at ROMO are generally expected to be related to air masses that are transported to the site from the NRFMA resulting from the mountain-plains solenoid circulation, a local transport phenomenon occurring frequently during summertime (Bossert and Cotton, 1994; Sullivan et al., 2016; Toth and Johnson, 1985). Such conditions have the potential to transport air pollutants into the park from oil and gas source regions as well as from urban sources across the Front Range, as shown in Figures 4 and 5. Conducting a similar back trajectory analysis for O_3 as done for the VOCs, Figure 10 shows results for HRT-ORT for the top 10% of O_3 measurements. As for the VOCs, elevated O_3 mixing ratios are largely associated with transport from the NFRMA (including Denver).

4.2 High O_3 Days

Impacts to ROMO during upslope events can be quite pronounced with elevated mixing ratios, but assessing these same upslope events averaged over a day or more diminishes their visibility resulting in lower overall values for these longer time periods. Therefore, we use an event based approach focused on upslope events from the NFRMA to examine what sources of Front Range emissions are impacting ROMO. During FRAPPÉ, 1-hr O_3 mixing ratios equal to or greater than 70 ppb were observed at both the ROMO-LP and ROMO-TR sites. These events are indicated by the grey shaded areas in Figure 3 and are summarized in Table 2. Elevated O_3 mixing ratios were typically accompanied by increased concentrations of various VOC source tracers. For example, alkyl nitrate concentrations (2-butyl nitrate, 2-BuONO$_2$, is shown as an example) in Figure 3 were elevated on six of the seven high O_3 days (not August 23). Alkyl nitrates are produced from the oxidation of

20

their parent hydrocarbons such as n-butane and n-pentane, emissions derived primarily from fossil fuels in the NFRMA, and share a common photochemical production mechanism with O_3. PAN was also elevated (>700 pptv) on all of the days shown in Table 2 except 23 and 24 August (see below).

During upslope flows created by thermally driven mountain-valley circulation, a mixture of direct emissions and photochemically produced secondary compounds can be transported to ROMO. We observed increases in concentration of a mixture of photochemically produced (PAN, alkyl nitrates) and directly emitted (alkanes, NO_x) compounds at ROMO during these events. The photochemistry that produces species like PAN and alkyl nitrates can occur anywhere along the transport path to the ROMO receptor site. VOC signatures are particularly useful in assessing the influence of oil and gas emissions in the Front Range on air masses with elevated O_3 mixing ratios transported to the park. As noted above, the i- to n-pentane ratio is expected to be less than one for air masses primarily impacted by oil and gas emissions. Two O_3 episodes, August 8 and August 18, occurred when the i- to n-pentane ratios were less than one at ROMO-LP (Table 2) together with elevated levels of alkyl nitrates. As seen in Figure 3, these dates also had some of the highest ethane mixing ratios observed throughout the study period, in addition to elevated mixing ratios of halocarbons, OVOCs, and ethyne. Although the air mass VOC signature does reflect several Front Range source types, it is dominated by oil and gas emissions as evidenced in the i-pentane to n-pentane ratio.

To further investigate the impact of VOCs on O_3 we next examine photochemical products and tracers. PAN is an excellent tracer of photochemical activity because it has a low background abundance and it is not directly emitted. Zaragoza et al. (2017) showed that when PAN and O_3 are disconnected in the Front Range, the source of the O_3 is not local photochemical production. At ROMO we see that increases in O_3 are associated with increases in alkyl nitrates and PAN suggesting a common photochemical source. Zaragoza et al. (2017) also showed that regional mixing is common during the most photochemically active summertime days in the Front Range. Emissions from multiple sources in the region are injected into air masses as they circulate in the Front Range and secondary species reflect production driven by a mix of sources. Peak PAN mixing ratios at BAO and ROMO were very similar on both August 8 and 18 (~800 pptv), supporting the assumption that mixed Front Range air pushed up into ROMO on these particular days. PAN/PPN (propionyl peroxynitrate) ratios at BAO during the afternoon on 18 August (high O_3 day at ROMO) ranged from 0.17 - 0.26. These relatively high ratios are indicative of a large PAN and

21

PPN source from the oxidation of alkanes from oil and gas production at BAO and throughout the region (Lindaas et al., submitted; Zaragoza et al., 2017). (2017) showed that when PAN and O₃ are disconnected in the Front Range, this indicates that the source of the O₃ is not local photochemical production. Zaragoza et al. (2017) also showed that regional mixing is common during the most photochemically active summertime days in the Front Range. Emissions from multiple sources in

5   the region are injected into air masses as they circulate in the Front Range and secondary species reflect production driven by a mix of sources. Peak PAN mixing ratios at BAO and ROMO were very similar on both August 8 and 18 (~800 pptv), supporting the assumption that mixed Front Range air pushed up into ROMO on these particular days. PAN/PPN (propionyl peroxynitrate) ratios at BAO during the afternoon on 18 August ranged from 0.17 - 0.26. Zaragoza et al. (2017) hypothesized that these relatively high ratios are indicative of a large PAN and PPN source from the oxidation of alkanes from oil and gas

10   production in the region, and this was recently verified by Lindaas et al. (submitted). Although PPN was not measured at ROMO, the high PAN/PPN ratio at BAO, the similar PAN mixing ratios between BAO and ROMO, and the high ethane mixing ratios at ROMO together suggest important contributions from oil and gas emissions to VOC signatures and O₃ on this date. Using a series of box model simulations, Lindaas et al. (submitted) tested the sensitivity of PAN and PPN production to a large set of possible NMHC precursors observed at BAO during summer 2015, and more generally showed that propane and

15   n-pentane are the dominant primary precursors for PPN in the Front Range.

Analogous to PAN, alkyl nitrates are photochemically produced simultaneously with ozone in the atmosphere. Here, we use We used coincident observations of alkyl nitrates during these elevated O₃ periods to estimate the contribution of the light alkanes emissions from oil and gas emissions to O₃ production. Alkyl nitrate formation can be used as a proxy for O₃ production if we make the following assumptions. First, their photochemical production is rapid compared to removal

20   processes and mixing across gradients. The rate of alkyl nitrate formation is tied to its parent alkane's concentration and reaction rate with the hydroxyl radical (OH), which is the hydroxyl radical reactivity (R1), as this is the rate limiting step in alkyl peroxy radical (RO₂) formation. In NFRMA areas that are influenced by oil and gas emissions, the hydroxyl radical reactivity values for the alkyl nitrate parent alkanes are high (Figure 11), resulting in rapid production compared to their removal rates. Because of their relatively long lifetimes (~ ≤10 days for summer), the C₂-C₅ alkyl nitrates can be transported

25   long distances and serve as a temporary reservoir for NOₓ, ultimately leading to O₃ production in downwind or remote regions

22

(e.g., Clemitshaw et al., 1997; Flocke et al., 1998; Roberts et al., 1998). For the upslope events on August 8 and 18, the assumption that photochemical production of the alkyl nitrates is rapid compared to removal processes is supported based on the rates of formation (hours) versus their removal (days). Second, the precursor compounds (VOCs and NO_x) both have sources in Weld County, where significant oil and gas development exists NO_x was elevated during both events (not shown) and the 2014 National Emissions Inventory (US EPA, 2017) suggests Weld County has the largest emissions of NO_x and VOCs in the state, and so it is reasonable to assume that emissions are collocated. The collocation of sources indicates these air masses likely contained sufficient NO_x for alkyl nitrate and O_3 formation and the excess O_3 is clearly related to VOC and NO_x emissions from the oil and gas region. There could be NO_x additions to the air mass as it moves west, but this does not violate the assumption because of the timescale for the transport, which is relatively fast. Third, transport time from the source region (NFRMA) to the park is rapid (on the order of hours). This assumption is validated by the time series plots shown in Figure 13, where during the upslope events, rapid increases in mixing ratios are observed within an hour of when the wind shifts to an upslope direction.

In general, this approach is similar to estimating O_3 production efficiency and background O_3 using O_x/NO_z but instead we use the individual alkyl nitrates in NO_z because of the abundance of alkanes emitted from oil and gas operations. Moreover, we can better apportion the photochemical processing from the source region emissions because we are using an ensemble of individual compounds that have known rate constants, branching ratios and processing times, as opposed to using a bulk parameter such as a NO_z, where the composition is not accurately known. For the oil and gas influenced upslope events at ROMO, PAN, O_3, NO_x, and alkyl nitrates all show coincident increases (Figure 3; Benedict et al., 2018). For the August 8 and 18 events, the overall air mass composition (Figures 3, 12, 1S and 2SFigure 11) and photochemical age (Figure 1312) indicate that the source region emissions and processing times in the Front Range were comparable and these assumptions are valid.

Because the production of O_3 and alkyl nitrates is tied to their common precursor, the alkyl peroxy radical (RO_2), correlation between O_3 and the C_2-C_5 alkyl nitrates is expected. As a first step, the y-intercept is used to estimate the background O_3 value for the event period prior to the start of the upslope event. As shown in Table 3, each of the individual alkyl nitrates gives a slightly different background O_3 value (y-intercept); however, they are all within a few ppbv of each

23

other, providing a reasonable estimate of the background O_3 during that time period.   The values reported for this work are also in the range of values reported by McDuffie et al. (2016) for BAO during summer 2014. The main source of the C_2-C_5 alkyl nitrates is the photochemical production from their parent alkane precursors, as outlined in the following simplified reaction scheme:

5

$$RH + OH \rightarrow R + H_2O \qquad (R1)$$

$$R + O_2 \rightarrow RO_2 \qquad (R2)$$

$$RO_2 + NO \rightarrow RO + NO_2 \qquad (R3a)$$

$$RO_2 + NO + M \rightarrow RONO_2 + M \qquad (R3b)$$

$$NO_2 + h\nu \rightarrow NO + O \qquad (R4)$$

10

$$O + O_2 + M \rightarrow O_3 + M \qquad (R5)$$

As shown by Reactions 1-5, alkyl nitrates share a common photochemical production mechanism with O_3. However, O_3 formation results from the photolysis of NO_2 (R4) whereas the formation of alkyl nitrates serve as a sink for NO_x, RO and RO_2, which affects O_3 production efficiency (Atkinson et al., 1982; Ranschaert et al., 2000; Russo et al., 2010b). Nonetheless, based on these reactions, it is expected that under a wide range of conditions O_3 and alkyl nitrates should be correlated as they

15 are produced concurrently in the atmosphere (e.g. Abeleira et al., 2018; Day et al., 2003; Flocke et al., 1991; Perring et al., 2013; Rosen et al., 2004; Russo et al., 2010b). Methyl nitrate is excluded from this analysis because photochemical production from its parent alkane, methane, does not meet our assumptions, and there are primary sources which impact the park (Benedict et al., 2018). For both of the oil and gas influenced upslope events, O_3 is plotted against each of the alkyl nitrates for the time periods immediately before and after the event, as shown in Figure 14 for 2-butyl nitrate. This relationship can be used to

20 provide a rough estimate of the excess O_3 associated with the upslope events transporting oil and gas impacted air masses from the NFRMA to the park. Using this method we can also investigate the contribution of other VOCs to O_3 production; however, in the case where alkanes are the dominant contributor to OH reactivity, we focus on the alkyl nitrates produced photochemically to provided an estimate of oil and gas impacts on O_3. As noted in Rosen et al. (2004), only a limited number of studies report the correlation of O_3 or O_x with alkyl nitrates, with half of the studies using the sum of alkyl nitrates (ΣANs)

25 because a non-selective technique was used that did not allow for individual speciation of the alkyl nitrates (Flocke et al., 1991;

Neuman et al., 2012; O'Brien et al., 1995; Perring et al., 2013; Roberts et al., 1996; Rosen et al., 2004). Flocke et al. (1991) reported the correlation of $\Sigma C_2–C_5$ straight chain alkane-derived nitrates plus a single C_4 branched chain alkane-derived nitrate with O_x measured at Shauinsland, Germany.

For both events (August 8 and 18), when the alkanes and OVOCs both contributed an average of 40% to OH reactivity, the average background O_3 was 43±2 ppbv. We use the background O_3 value to estimate ~~Because the production of O_3 and alkyl nitrates are tied to their common precursor, the alkyl peroxy radical (RO₂), correlation between O₃ and the C₂-C₅ alkyl nitrates is expected. Methyl nitrate is excluded from this analysis because photochemical production from its parent alkane, methane, does not meet our assumptions, and there are primary sources which impact the park (Benedict et al., in review). For both of the oil and gas influenced events, O₃ is plotted against each of the alkyl nitrates for the time periods immediately before and after the event, as shown in Figure 13 for 2-butyl nitrate. This relationship can be used to provide an estimate of the excess O₃ produced resulting from the upslope events transporting oil and gas impacted air masses from the NFRMA to the park. As a first step, the y-intercept is used to estimate the background O₃ value for the event period. As shown in Table 3, each of the individual alkyl nitrates gives a slightly different background O₃ value (y-intercept); however, they are all within a few ppbv of each other, providing a reasonable best estimate of the background O₃ during that time period. For both events, August 8 and August 18, the average background O₃ was 43±2 ppbv. This is in the range of values reported by McDuffie et al. (2016) for BAO during summer 2014.~~

~~We use these background O_3 values to aid in bracketing~~ the range of influence on O_3 production derived from oil and gas emissions driven by the individual parent alkane~~NMHC~~ precursors (attributed O_3). To this end, the orthogonal distance linear regressions between O_3 and each of the individual C_2-C_5 alkyl nitrates are used. To estimate the excess O_3 produced and transported to ROMO during the upslope events, the slope of O_3 versus each of the alkyl nitrates was determined, then the hourly concentration for each alkyl nitrate was multiplied by the slope value and the intercept value was subtracted. Table 3 provides a summary of the O_3/$RONO_2$ slopes in ppbv/ppbv, intercept values (background O_3) in ppbv, the range of attributed O_3 (ppbv), and the attributed O_3 value (ppbv) based on the correlation in each of the O_3-alkyl nitrate scatter plots. The estimated average attributed O_3 production values determined for each event are 22±3 ppbv and 19±2 ppbv for the August 8 and August 18 events at ROMO-LP, respectively. These values represent an upper limit on the excess O_3 produced from NFRMA air

masses transported to ROMO that were dominated by oil and gas emissions. Other compounds produced photochemically in situ (e.g., PAN and acetone) provide similar values to the alkyl nitrates for the attributed O_3 (not shown). The alkyl nitrate correlation method does not allow us to explicitly separate the impact of NO_x, additional OVOCs or other species such as alkenes (Figure 11), which all likely contribute to ozone production. These results are consistent with measurements along the NFRMA during FRAPPÉ by Cheadle et al. (2017), who showed that on individual days emissions from oil and gas operations can contribute upwards of 30 ppbv to excess O_3 production. The high concentration air masses measured in the Front Range contain a similar mix of compounds as the air masses transported to ROMO during upslope events. Accounting for mixing and dilution, enhancements in O_3 resulting from oil and gas emissions are expected to be lower at ROMO. Worth noting is the consistency of these O_3 enhancements for the two events at ROMO and the marked similarity of the air mass compositions measured in the park (Figure 12~~14~~). Figure 12~~14~~ shows O_3, ethane and alkyl nitrate mixing ratios during the events, along with meteorology data. For the August 8 upslope event, the winds were variable and out of the SSE and it was sunnier (solar radiation ~200-300 W m^{-2} higher) than August 18, but ~3 °C cooler (not shown). The August 18 upslope event had winds from the east and a sharp drop in solar radiation just prior to the upslope event. Nonetheless, the alkyl nitrates, light alkanes, PAN, and O_3 mixing ratios were strikingly comparable during these two events (Figure 12~~14~~) as were the overall air mass reactivity~~composition~~ (Figure 11) and photochemical age (Figure 13~~12~~), indicating comparable source region emissions. ~~, as indicated by the dominant oil and gas signature and the photochemical processing times.~~ When considering the entire study period, and not just these specific events, the oil and gas contribution to O_3 at ROMO is much smaller than during these episodes, given that upslope (south easterly) flow is not the predominant wind direction (McDuffie et al., 2016).

Intermediate i- to n-pentane ratios (1.12-1.44) were observed for measurements on July 22, August 11, and August 12, suggesting that multiple Front Range sources impacted ROMO during these O_3 events. In addition to urban sources, biomass burning emissions influenced the Front Range on August 11-12 (Dingle et al., 2016). The highest O_3 levels across the Front Range during FRAPPÉ were observed on July 22 (Pfister et al., 2017; Sullivan et al., 2016), which also had the highest average afternoon (12:00-20:00) concentrations of total alkanes (9700 pptv), alkenes (277 pptv), biogenics (252 pptv), alkyl nitrates (110 pptv), and OVOCs (9.8 ppbv; methanol, acetaldehyde, MVK+MACR, MEK, and acetic acid) at ROMO among all of the high O_3 days. Throughout the region, clear skies and a lower and slow growing planetary boundary layer,

26

coupled with reduced ventilation, resulted in less dilution and increased precursor concentrations, contributing to the elevated O_3 (Pfister et al., 2017). These elevated mixing ratios were likely then transported to ROMO by thermally driven upslope flow observed along the Front Range (Sullivan et al., 2016).

The O_3 events observed on August 23 (ROMO-LP) and August 24 (ROMO-TR) have neither an oil and gas nor an urban signature. PAN also remained < 300 pptv during both days. Here we focus on the event on August 23 at ROMO-LP, where VOC measurements were collocated. On August 23, air masses came from the west without passing over the NFRMA and had much lower abundances of O_3 precursors and photochemical products (Figure 3), suggesting that the high O_3 mixing ratios were not generated from regional photochemical production. These high O_3 mixing ratios are associated with the red region in western Colorado in Figure 10. Mixing ratios of alkanes (total 1505 pptv), alkenes (total 93 pptv), aromatics (42 pptv), alkyl nitrates (total 17 ppt), halocarbons (4 pptv; C_2Cl4, CH_3I, CH_2Br_2, $CHBrCl_2$, CHBr3), and OVOCs (2.8 ppbv; methanol, acetaldehyde, MVK+MACR, MEK, and acetic acid) were all low compared to the other high O_3 periods and most of the study. For this same time period the average NO_x mixing ratio (0.52 ppbv) was lower than those during other high O_3 periods (1.2-3.1 ppbv; no data for August 11).   Additionally, a comparison of soundings from Denver (http://weather.uwyo.edu/upperair/sounding.html) shows a pocket of dry air from 500 to 100 hPa which ~~doesn't~~ does not occur on any of the other high O_3 days (Figure 15a), and water vapour decreases during the event on August 23 (Figure 15b). This is the only high O_3 event for which O_3 and water vapour exhibit a robust anti-correlation (R^2=0.627, p<0.0001) during the study. The low coincident mixing ratios of NO_x and VOCs, the dry air aloft, and the robust anti-correlation of O_3 and water vapour at the surface during the O_3 event suggest an intrusion of stratospheric or upper tropospheric air on August 23. A stratospheric-tropospheric exchange event also was observed in Fort Collins in early August during FRAPPÉ (Sullivan et al., 2016).

4.3 Hydroxyl Radical (OH) Reactivity and Photochemical Age

Photolysis of NO_2 is the only way to produce O_3 in the troposphere. Oxidation of VOCs by hydroxyl radicals (OH) in the atmosphere is typically the first step in the formation of peroxy radicals (RO_2) which react with NO to produce NO_2. Calculating the kinetic OH reactivity (OHR) helps to identifiy compounds that are likely to quickly form RO_2 and ultimately~~ultimatly~~ contribute to O_3 production. The OHR for ~~NMHCs~~ VOCs is calculated using the following expression:

27

$$OHR = \sum [\text{NMHC} VOC]_i \times k_{\text{NMHC} VOC_{i+OH}} \quad \text{Eq. (1)}$$

where [~~NMHC~~VOC]$_i$ is the concentration of each ~~NMHC~~ VOC and $k_{\text{NMHC} VOC_{i+OH}}$ is the reaction rate constant for each ~~NMHC~~

VOC with OH. The OHR is calculated for the high O$_3$ events during FRAPPÉ which had an oil and gas influence, a combined

oil and gas and urban influence, the stratospheric/upper troposphere intrusion event, and for background conditions (without

5   regard to the O$_3$ mixing ratio and defined as lowest 10th percentile for ethane). This metric is an imperfect measure of O$_3$

production potential since it does not account for chain termination or propagation steps, nor does it properly capture

differences in VOC production of peroxy radicals during photolysis or reaction with other oxidants. However, OHR is a useful

tool because it is a measure of the initial rate of peroxy radical formation that can be interpreted as the potential for a specific

compound to ultimately produce O$_3$.

10   For the events influenced by oil and gas emissions, the alkanes and OVOCs were the major contributors~~contributor~~

to the ~~NMHC~~VOC-OHR, comprising almost 40% and 39%, respectively,~~70%~~ of the calculated total (Figure 11). For the high

O$_3$ air masses that also included an urban influence, the OHR for OVOCs dominated (40%), followed by ~~alkenes (~28%) and~~

alkanes (~20%) and alkenes (~17%) which~~37%)~~ were more comparable, reflecting increased reactivity contributions of the

light alkenes from urban areas. However, the alkanes were still the largest non-OVOC contributor of OH reactivity to this

15   category. The importance of isoprene, with ~21~~32~~% of the total reactivity, is also more apparent, even though the average

mixing ratio was only 64 pptv for these days. ~~Interestingly, the overall background NMHC-OHR (0.86 s⁻¹) was comparable~~

~~to that of the oil and gas influenced days (0.90 s⁻¹ OHR).~~ Larger mixing ratios of isoprene (~270 pptv) during background

periods results in the calculated ~~NMHC~~VOC-OHR being dominated (~74~~86~~%) by isoprene reactivity and of similar

magnitutude as the more polluted oil and gas days. In all cases, ethyne and the aromatics were only minor contributors to the

20   calculated overall OHR. Finally, it is worth noting that the OHR values calculated here are lower bounds on the actual VOC-

OHR in the studied air masses. The OHR values only represent the initial attack of OH with the ~~NMHC~~ VOC and does not

reflect ~~does not consider~~ the subsequent contributions of the oxidation products formed and how these influence and change

the overall air mass and its reactivity. ~~As Abeleira et al. (2017) points out for measurements at BAO, other VOC classes not~~

~~included in the ROMO analysis (e.g., oxygenated VOCs) are also significant contributors to total VOC OHR.~~

To estimate the impact of the oil and gas emissions on OHR at the park, we compare the average straight chain alkane OHR during the upslope events to that of the background and combined oil and gas and urban-influenced alkane OHRs, which include the C_2-C_8 alkanes. The reactivity attributed to the alkanes is considered because they are the dominant VOCs associated with the oil and gas emissions. The alkane OHR for the oil and gas events was 0.62 s^{-1}, which comprised ~40% of the total

5   calculated OHR (includes all measured compounds) for those events. In comparison to the oil and gas influenced events, the alkane OHR for the urban-influenced events was only 0.21 s^{-1}, while the background alkane OHR was only 0.02 s^{-1}, and comprised much smaller fractions of the total calculated OHR for those periods. The difference in alkane reactiviy between the oil and gas events and the urban-influenced events was 0.41 s^{-1}; the difference between oil and gas influenced and background events was 0.60 s^{-1}. Furthermore, the percent contribution of the individual straight chain C_2-C_8 alkanes to the

10   total alkane OHR is similar to that of other measurements made in the regions across seasons (Abeleira et al., 2017; Halliday et al., 2016; McDuffie et al., 2016; Swarthout et al., 2013) underscoring the consistent temporal and spatial compositional influence of the oil and gas source signature impacting ROMO during upslope events (Table 4).

Air mass photochemical age can be calculated using the alkyl nitrate to parent hydrocarbon ratio (R-ONO$_2$/R-H) (e.g. Bertman et al., 1995; Russo et al., 2010b; Simpson et al., 2003; Swarthout et al., 2013). This reaction scheme assumes only

15   OH-initiated photochemical production of a given alkyl nitrate from its parent hydrocarbon, and so deviations from the model suggest additional sources or chemistry not captured in this simple scheme. Details of the chemical mechanisms and calculations can be found in the supplement. The modelled ratios of 3-pentyl nitrate to n-pentane versus 2-butyl nitrate to n-butane are calculated using [OH] = 10^6 molecules cm^{-3} and are shown as the solid line in Figure 13$\cancel{12}$. Measured ratios of these species are shown as the symbols and are coloured by O$_3$ mixing ratio. Based on this model, VOC ages in sampled air

20   masses ranged from several hours to two days and, as generally observed with the pentyl nitrates, they typically lie below the model prediction line with a relatively small offset. Focusing on the high O$_3$ periods, shown as red filled symbols, the oil and gas influenced events on August 8 and August 18 show the best agreement with the model, with a photochemical age of less than one day, indicating local sources of the parent hydrocarbons and that photochemical production was driving the O$_3$ and alkyl nitrate production these days. On July 22, August 11 and August 12, when both urban and oil and gas impacts were

25   observed, the measured ratios deviate from the model in a systematic way, suggesting that the air masses were influenced by

multiple chemical processes. Finally, on August 23 and 24, the alkyl nitrate to parent alkane ratios deviated from the photochemical line significantly, providing another line of evidence that the increase in O_3 was not from photochemical production in a polluted environment, consistent with influences of O_3 enriched air from the upper troposphere.

5. Summary and Conclusions

5   Rocky Mountain National Park is a Class I area that is afforded the highest level of air quality protection. Nevertheless, O_3 mixing ratios can reach levels that negatively impact vegetation and human health, particularly for older adults and people who are active outdoors. In this study, O_3 and a suite of VOC measurements were made at ROMO as part of the 2014 FRAPPÉ field campaign. Although average and peak O_3 mixing ratios were lower during FRAPPÉ compared to other recent summer seasons, one-hour mixing ratios exceeding 70 ppbv routinely measured in the park during this period.

10   This study was aimed at better understanding sources of VOCs that impact the park and, particularly, what drives these high ozone events.

ROMO is located just west of the NFRMA in Colorado, and the park can be impacted by a variety of emissions sources. Significant variability in the measured VOC abundances suggest that the sampling site was impacted by emissions from biogenic, urban, combustion, agricultural, and oil and gas sources during the study period. Light alkanes measured at

15   ROMO, markers for oil and gas production, were significantly elevated relative to background levels, and at times reached mixing ratios measured in some oil and gas source regions during upslope events (e.g., Swarthout et al, 2015). Mixing ratios reached 9800 ppt for ethane, 1158 ppt for i-butane, 2378 ppt for n-butane, 2095 ppt for i-pentane, and 1712 ppt for n-pentane.

Using VOCs as source markers, we determined that the elevated O_3 periods were primarily associated with upslope events. For the oil and gas impacted days, <u>Front Range emissions</u>~~light alkanes~~ contributed <u>an upper bound of</u>~~approximately~~ 20 ppbv

20   excess O_3, having a major impact on total O_3 mixing ratios on those days. In air masses with increased urban influence, alkenes played a more important role; however, even for these urban influenced air masses, a clear oil and gas signature was also present. During background periods, when air masses arrived from the west, O_3 was typically low and ~~NMHC~~<u>VOC</u> -OH reactivity was dominated by isoprene (<u>74</u>~~86~~%). Total ~~NMHC~~<u>VOC</u>-OHR was of similar magntitude on the background (<u>0.99</u>~~0.86~~ s^{-1}) and oil and gas influenced (<u>1.26s</u>~~0.895 s~~$^{-1}$) days but alkanes dominated total ~~NMHC~~<u>VOC</u>-OHR (<u>40</u>~~69~~%) on oil

and gas days. The mixed urban and oil and gas influenced days were characterized by slightly lower total ~~NMHC~~VOC-OHR

(0.~~825~~546 s^{-1}) and OH reactivity was dominated by OVOCs (40%), alkanes (20~~37~~%) and alkenes (17~~28~~%). In one distinct

case, elevated O_3 was associated with air mass transport from the west. For this case, the abundances of VOCs and other

secondary species were very low (Total ~~NMHC~~VOC-OHR =0.~~16s~~07s^{-1}), and there was a clear anti-correlation of O_3 and

5   surface water vapour, suggesting that an intrusion of stratospheric or O_3-rich upper-tropospheric air contributed to elevated O_3

measured at the surface.

Elevated O_3 in the Front Range and ROMO has been a persistent air quality issue. Findings from this study reaffirm

that ROMO is impacted by a variety of anthropogenic emissions sources in the NFRMA. State and federal agencies have

implemented regulations that have successfully reduced emissions from traditional sources (mobile, power plant, and other

10   activities) gradually reducing O_3 since 2009 at a rate of -0.25 $\pm$ 0.13 ppbv yr^{-1} in ROMO (McGlynn et al., 2018)~~(McGlynn et~~

~~al., 2018)~~. Continued population growth and the competing effects of increasing emissions from oil and gas extraction appear

to be diminishing the impact of the regulations as emissions from emerging sectors or increased population are contributing to

the high O_3 episodes. Management practices aimed at reducing high O_3 levels at the park thus cannot focus on controlling a

single source, but instead must take a broader approach to focus on reductions in the traditional sources as well as these new

15   sources. Recent work by Zhou et al. (in prep)~~(in prep)~~ suggest that emission reductions of both volatile organic compounds

(VOCs) and nitrogen oxides (NO_x) could lead to effective O_3 mitigation in the Intermountain West. Additionally, identifying

periods of stratospheric O_3 influence should also be a priority when assessing which high O_3 episodes can be mitigated through

emissions control.

Data Availability

20   The data used in this analysis are available in the FRAPPÉ/DISCOVER-AQ data archive (https://www-air.larc.nasa.gov/cgi-
bin/ArcView/discover-aq.co-2014) in the Ground-Other category under the PIs Collett, Fischer, and Sive.

5

References

Abeleira, A., Pollack, I. B., Sive, B., Zhou, Y., Fischer, E. V. and Farmer, D. K.: Source characterization of volatile organic compounds in the Colorado Northern Front Range Metropolitan Area during spring and summer 2015, J. Geophys. Res. Atmospheres, 122(6), 3595–3613,
10   doi:10.1002/2016JD026227, 2017.

Abeleira, A., Sive, B., Swarthout, R. F., Fischer, E. V., Zhou, Y. and Farmer, D. K.: Seasonality, sources and sinks of C_1–C_5 alkyl nitrates in the Colorado Front Range, Elem Sci Anth, 6(1), doi:10.1525/elementa.299, 2018.

Ashbaugh, L. L., Malm, W. C. and Sadeh, W. Z.: A residence time probability analysis of sulfur
15   concentrations at Grand Canyon National Park, Atmospheric Environ. 1967, 19(8), 1263–1270, doi:10.1016/0004-6981(85)90256-2, 1985.

ASTM Standard D1835-16: Standard Specification for Liquefied Petroleum (LP) Gases, ASTM International, West Conshohocken, PA. [online] Available from: www.astm.org (Accessed 17 July 2018), 2016.

20   Atkinson, R.: Kinetics and mechanisms of the gas-phase reactions of the hydroxyl radical with organic compounds under atmospheric conditions, Chem. Rev., 86(1), 69–201, doi:10.1021/cr00071a004, 1986.

Atkinson, R. and Arey, J.: Atmospheric Degradation of Volatile Organic Compounds, Chem. Rev., 103(12), 4605–4638, doi:10.1021/cr0206420, 2003.

Atkinson, R., Aschmann, S. M., Carter, W. P. L., Winer, A. M. and Pitts, J. N.: Alkyl nitrate formation
25   from the nitrogen oxide (NOx)-air photooxidations of C2-C8 n-alkanes, J. Phys. Chem., 86(23), 4563–4569, doi:10.1021/j100220a022, 1982.

Baker, A. K., Beyersdorf, A. J., Doezema, L. A., Katzenstein, A., Meinardi, S., Simpson, I. J., Blake, D. R. and Sherwood Rowland, F.: Measurements of nonmethane hydrocarbons in 28 United States cities, Atmos. Environ., 42(1), 170–182, doi:10.1016/j.atmosenv.2007.09.007, 2008.

Beem, K. B., Raja, S., Schwandner, F. M., Taylor, C., Lee, T., Sullivan, A. P., Carrico, C. M., McMeeking, G. R., Day, D., Levin, E., Hand, J., Kreidenweis, S. M., Schichtel, B., Malm, W. C. and Collett, J. L.: Deposition of reactive nitrogen during the Rocky Mountain Airborne Nitrogen and Sulfur (RoMANS) study, Environ. Pollut., 158(3), 862–872, doi:10.1016/j.envpol.2009.09.023, 2010.

5   Benedict, K. B., Day, D., Schwandner, F. M., Kreidenweis, S. M., Schichtel, B., Malm, W. C. and Collett, J. L.: Observations of atmospheric reactive nitrogen species in Rocky Mountain National Park and across northern Colorado, Atmos. Environ., 64, 66–76, doi:10.1016/j.atmosenv.2012.08.066, 2013.

Benedict, K. B., Prenni, A. J., Sullivan, A. P., Evanoski-Cole, A. R., Fischer, E. V., Callahan, S., Sive, B. C., Zhou, Y., Schichtel, B. A. and Jr, J. L. C.: Impact of Front Range sources on reactive nitrogen
10 concentrations and deposition in Rocky Mountain National Park, PeerJ, 6, e4759, doi:10.7717/peerj.4759, 2018.

Bertman, S. B., Roberts, J. M., Parrish, D. D., Buhr, M. P., Goldan, P. D., Kuster, W. C., Fehsenfeld, F. C., Montzka, S. A. and Westberg, H.: Evolution of alkyl nitrates with air mass age, J. Geophys. Res. Atmospheres, 100(D11), 22805–22813, doi:10.1029/95JD02030, 1995.

15 Blake, D. R., Blake, N. J., Smith, T. W., Wingenter, O. W. and Rowland, F. S.: Nonmethane hydrocarbon and halocarbon distributions during Atlantic Stratocumulus Transition Experiment/Marine Aerosol and Gas Exchange, June 1992, J. Geophys. Res. Atmospheres, 101(D2), 4501–4514, doi:10.1029/95JD01370, 1996.

Bossert, J. E. and Cotton, W. R.: Regional-Scale Flows in Mountainous Terrain. Part I: A Numerical
20 and Observational Comparison, Mon. Weather Rev., 122(7), 1449–1471, doi:10.1175/1520-0493(1994)122<1449:RSFIMT>2.0.CO;2, 1994.

Cheadle, L. C., Oltmans, S. J., Petron, G., Schnell, R. C., Mattson, E. J., Herndon, S. C., Thompson, A. M., Blake, D. R. and McClure-Begley, A.: Surface ozone in the Colorado northern Front Range and the influence of oil and gas development during FRAPPE/DISCOVER-AQ in summer 2014, Elem Sci
25 Anth, 5(0), doi:10.1525/elementa.254, 2017.

Christensen, J. N., Weiss-Penzias, P., Fine, R., McDade, C. E., Trzepla, K., Brown, S. T. and Gustin, M. S.: Unraveling the sources of ground level ozone in the Intermountain Western United States using Pb isotopes, Sci. Total Environ., 530–531, 519–525, doi:10.1016/j.scitotenv.2015.04.054, 2015.

COGCC: Greater Wattenberg Area Baseline Study, Technical Report, Colorado Oil and Gas
30 Conservation Commission., 2007.

COGCC: Well Surface Location Data, CO Oil and Gas Conservation Commission. [online] Available from: http://cogcc.state.co.us/data2.html#/downloads (Accessed 24 January 2018), 2018.

Day, D. A., Dillon, M. B., Wooldridge, P. J., Thornton, J. A., Rosen, R. S., Wood, E. C. and Cohen, R. C.: On alkyl nitrates, O3, and the "missing NOy," J. Geophys. Res. Atmospheres, 108(D16), 4501, doi:10.1029/2003JD003685, 2003.

Dingle, J. H., Vu, K., Bahreini, R., Apel, E. C., Campos, T. L., Flocke, F., Fried, A., Herndon, S., Hills, A. J., Hornbrook, R. S., Huey, G., Kaser, L., Montzka, D. D., Nowak, J. B., Reeves, M., Richter, D., Roscioli, J. R., Shertz, S., Stell, M., Tanner, D., Tyndall, G., Walega, J., Weibring, P. and Weinheimer, A.: Aerosol optical extinction during the Front Range Air Pollution and Photochemistry Éxperiment (FRAPPÉ) 2014 summertime field campaign, Colorado, USA, Atmospheric Chem. Phys., 16(17), 11207–11217, doi:10.5194/acp-16-11207-2016, 2016.

Flocke, F., Volz-Thomas, A. and Kley, D.: Measurements of alkyl nitrates in rural and polluted air masses, Atmospheric Environ. Part Gen. Top., 25(9), 1951–1960, doi:10.1016/0960-1686(91)90276-D, 1991.

Gebhart, K. A., Schichtel, B. A., Malm, W. C., Barna, M. G., Rodriguez, M. A. and Collett, J. L.: Back-trajectory-based source apportionment of airborne sulfur and nitrogen concentrations at Rocky Mountain National Park, Colorado, USA, Atmos. Environ., 45(3), 621–633, doi:10.1016/j.atmosenv.2010.10.035, 2011.

Gebhart, K. A., Malm, W. C., Rodriguez, M. A., Barna, M. G., Schichtel, B. A., Benedict, K. B., Collett, J. L. and Carrico, C. M.: Meteorological and Back Trajectory Modeling for the Rocky Mountain Atmospheric Nitrogen and Sulfur Study II, Adv. Meteorol., 2014, 1–19, doi:10.1155/2014/414015, 2014.

Gilman, J. B., Lerner, B. M., Kuster, W. C. and de Gouw, J. A.: Source Signature of Volatile Organic Compounds from Oil and Natural Gas Operations in Northeastern Colorado, Environ. Sci. Technol., 47(3), 1297–1305, doi:10.1021/es304119a, 2013.

Halliday, H. S., Thompson, A. M., Wisthaler, A., Blake, D. R., Hornbrook, R. S., Mikoviny, T., Müller, M., Eichler, P., Apel, E. C. and Hills, A. J.: Atmospheric benzene observations from oil and gas production in the Denver-Julesburg Basin in July and August 2014, J. Geophys. Res. Atmospheres, 121(18), 2016JD025327, doi:10.1002/2016JD025327, 2016.

Harley, R. A., Hannigan, M. P. and Cass, G. R.: Respeciation of organic gas emissions and the detection of excess unburned gasoline in the atmosphere, Environ. Sci. Technol., 26(12), 2395–2408, doi:10.1021/es00036a010, 1992.

Janjic, Z. I.: A nonhydrostatic model based on a new approach, Meteorol. Atmospheric Phys., 82(1–4), 271–285, doi:10.1007/s00703-001-0587-6, 2003.

Jobson, B. T., Wu, Z., Niki, H. and Barrie, L. A.: Seasonal trends of isoprene, C2–C5 alkanes, and acetylene at a remote boreal site in Canada, J. Geophys. Res. Atmospheres, 99(D1), 1589–1599, doi:10.1029/93JD00424, 1994.

Kohut, R., Flanagan, C., Cheatham, J. and Porter, E.: Foliar Ozone Injury on Cutleaf Coneflower at
5 Rocky Mountain National Park, Colorado, West. North Am. Nat., 72(1), 32–42, doi:10.3398/064.072.0104, 2012.

Koppmann, R., Ed.: Volatile Organic Compounds in the Atmosphere, 1 edition., Wiley-Blackwell, Oxford ; Ames, Iowa., 2007.

Lin, M., Fiore, A. M., Horowitz, L. W., Langford, A. O., Oltmans, S. J., Tarasick, D. and Rieder, H. E.:
10 Climate variability modulates western US ozone air quality in spring via deep stratospheric intrusions, Nat. Commun., 6, 7105, doi:10.1038/ncomms8105, 2015.

Lindaas, J., Farmer, D. K., Pollack, I. B., Abeleira, A., Flocke, F. and Fischer, E. V.: Acyl peroxy nitrates link oil and natural gas emissions to high ozone abundances in the Colorado Front Range during summer 2015, J. Geophys. Res.-Atmospheres, submitted.

15 McDuffie, E. E., Edwards, P. M., Gilman, J. B., Lerner, B. M., Dubé, W. P., Trainer, M., Wolfe, D. E., Angevine, W. M., deGouw, J., Williams, E. J., Tevlin, A. G., Murphy, J. G., Fischer, E. V., McKeen, S., Ryerson, T. B., Peischl, J., Holloway, J. S., Aikin, K., Langford, A. O., Senff, C. J., Alvarez, R. J., Hall, S. R., Ullmann, K., Lantz, K. O. and Brown, S. S.: Influence of oil and gas emissions on summertime ozone in the Colorado Northern Front Range, J. Geophys. Res. Atmospheres, 121(14),
20 2016JD025265, doi:10.1002/2016JD025265, 2016.

McGaughey, G. R., Desai, N. R., Allen, D. T., Seila, R. L., Lonneman, W. A., Fraser, M. P., Harley, R. A., Pollack, A. K., Ivy, J. M. and Price, J. H.: Analysis of motor vehicle emissions in a Houston tunnel during the Texas Air Quality Study 2000, Atmos. Environ., 38(20), 3363–3372, doi:10.1016/j.atmosenv.2004.03.006, 2004.

25 McGlynn, D., Mao, H., Wu, Z., Sive, B. and Sharac, T.: Understanding Long-Term Variations in Surface Ozone in United States (U.S.) National Parks, Atmosphere, 9(4), 125, doi:10.3390/atmos9040125, 2018.

McLaren, R., Singleton, D. L., Lai, J. Y. K., Khouw, B., Singer, E., Wu, Z. and Niki, H.: Analysis of motor vehicle sources and their contribution to ambient hydrocarbon distributions at urban sites in
30 Toronto during the Southern Ontario oxidants study, Atmos. Environ., 30(12), 2219–2232, doi:10.1016/1352-2310(95)00178-6, 1996.

Musselman, R. C. and Korfmacher, J. L.: Ozone in remote areas of the Southern Rocky Mountains, Atmos. Environ., 82, 383–390, doi:10.1016/j.atmosenv.2013.10.051, 2014.

National Park Service: Stats Report Viewer, [online] Available from:
https://irma.nps.gov/Stat/Reports/Park (Accessed 3 February 2017), 2017.

Neuman, J. A., Aikin, K. C., Atlas, E. L., Blake, D. R., Holloway, J. S., Meinardi, S., Nowak, J. B.,
Parrish, D. D., Peischl, J., Perring, A. E., Pollack, I. B., Roberts, J. M., Ryerson, T. B. and Trainer, M.:
5 Ozone and alkyl nitrate formation from the Deepwater Horizon oil spill atmospheric emissions:
OZONE AND ALKYL NITRATES FROM DWH, J. Geophys. Res. Atmospheres, 117(D9), n/a-n/a,
doi:10.1029/2011JD017150, 2012.

O'Brien, J., Shepson, P., Muthuramu, K., Hao, C., Niki, H., Hastie, D., Taylor, R. and Roussel, P.:
Measurements of Alkyl and Multifunctional Organic Nitrates at a Rural Site in Ontario, J. Geophys.
10 Res.-Atmospheres, 100(D11), 22795–22804, doi:10.1029/94JD03247, 1995.

Parrish, D. D., Trainer, M., Young, V., Goldan, P. D., Kuster, W. C., Jobson, B. T., Fehsenfeld, F. C.,
Lonneman, W. A., Zika, R. D., Farmer, C. T., Riemer, D. D. and Rodgers, M. O.: Internal consistency
tests for evaluation of measurements of anthropogenic hydrocarbons in the troposphere, J. Geophys.
Res. Atmospheres, 103(D17), 22339–22359, doi:10.1029/98JD01364, 1998.

15 Perring, A. E., Pusede, S. E. and Cohen, R. C.: An Observational Perspective on the Atmospheric
Impacts of Alkyl and Multifunctional Nitrates on Ozone and Secondary Organic Aerosol, Chem. Rev.,
113(8), 5848–5870, doi:10.1021/cr300520x, 2013.

Pétron, G., Frost, G., Miller, B. R., Hirsch, A. I., Montzka, S. A., Karion, A., Trainer, M., Sweeney, C.,
Andrews, A. E., Miller, L., Kofler, J., Bar-Ilan, A., Dlugokencky, E. J., Patrick, L., Moore, C. T.,
20 Ryerson, T. B., Siso, C., Kolodzey, W., Lang, P. M., Conway, T., Novelli, P., Masarie, K., Hall, B.,
Guenther, D., Kitzis, D., Miller, J., Welsh, D., Wolfe, D., Neff, W. and Tans, P.: Hydrocarbon
emissions characterization in the Colorado Front Range: A pilot study, J. Geophys. Res. Atmospheres,
117(D4), D04304, doi:10.1029/2011JD016360, 2012.

Pfister, G. G., Reddy, P. J., Barth, M. C., Flocke, F. F., Fried, A., Herndon, S. C., Sive, B. C., Sullivan,
25 J. T., Thompson, A. M., Yacovitch, T. I., Weinheimer, A. J. and Wisthaler, A.: Using Observations and
Source-Specific Model Tracers to Characterize Pollutant Transport During FRAPPÉ and DISCOVER-
AQ, J. Geophys. Res. Atmospheres, 122(19), 2017JD027257, doi:10.1002/2017JD027257, 2017.

Poirot, R. L., Wishinski, P. R., Hopke, P. K. and Polissar, A. V.: Comparative Application of Multiple
Receptor Methods To Identify Aerosol Sources in Northern Vermont, Environ. Sci. Technol., 35(23),
30 4622–4636, doi:10.1021/es010588p, 2001.

Prenni, A. J., Day, D. E., Evanoski-Cole, A. R., Sive, B. C., Hecobian, A., Zhou, Y., Gebhart, K. A.,
Hand, J. L., Sullivan, A. P., Li, Y., Schurman, M. I., Desyaterik, Y., Malm, W. C., Collett Jr., J. L. and
Schichtel, B. A.: Oil and gas impacts on air quality in federal lands in the Bakken region: an overview
of the Bakken Air Quality Study and first results, Atmos Chem Phys, 16(3), 1401–1416,
35 doi:10.5194/acp-16-1401-2016, 2016.

Ranschaert, D. L., Schneider, N. J. and Elrod, M. J.: Kinetics of the $C_2H_5O_2 + NO_x$ Reactions: Temperature Dependence of the Overall Rate Constant and the $C_2H_5ONO_2$ Branching Channel of $C_2H_5O_2 + NO$, J. Phys. Chem. A, 104(24), 5758–5765, doi:10.1021/jp000353k, 2000.

Reddy, P. J. and Pfister, G. G.: Meteorological factors contributing to the interannual variability of midsummer surface ozone in Colorado, Utah, and other western U.S. states, J. Geophys. Res. Atmospheres, 121(5), 2015JD023840, doi:10.1002/2015JD023840, 2016.

Rindsland, C. P., Jones, N. B., Connor, B. J., Wood, S. W., Goldman, A., Stephen, T. M., Murcray, F. J., Chiou, L. S., Zander, R. and Mahieu, E.: Multiyear infrared solar spectroscopic measurements of HCN, CO, C2H6, and C2H2 tropospheric columns above Lauder, New Zealand (45°S latitude), Journal of Geophysical Research: Atmospheres [online] Available from: https://agupubs.onlinelibrary.wiley.com/doi/abs/10.1029/2001JD001150 (Accessed 14 August 2018), 2002.

Roberts, J. M., Parrish, D., Norton, R. B., Bertman, S. B., Holloway, J. S., Trainer, M., Fehsenfeld, F. C., Carroll, M. A., Albercook, G. M., Wang, T. and Forbes, G.: Episodic removal of NOy species from the marine boundary layer over the North Atlantic, J. Geophys. Res.-Atmospheres, 101(D22), 28947–28960, 1996.

Rosen, R. S., Wood, E. C., Wooldridge, P. J., Thornton, J. A., Day, D. A., Kuster, W., Williams, E. J., Jobson, B. T. and Cohen, R. C.: Observations of total alkyl nitrates during Texas Air Quality Study 2000: Implications for O3 and alkyl nitrate photochemistry, J. Geophys. Res. Atmospheres, 109(D7), D07303, doi:10.1029/2003JD004227, 2004.

Rudolph, J.: The tropospheric distribution and budget of ethane, Journal of Geophysical Research: Atmospheres [online] Available from: https://agupubs.onlinelibrary.wiley.com/doi/abs/10.1029/95JD00693 (Accessed 14 August 2018), 1995.

Russo, R. S., Zhou, Y., White, M. L., Mao, H., Talbot, R. and Sive, B. C.: Multi-year (2004–2008) record of nonmethane hydrocarbons and halocarbons in New England: seasonal variations and regional sources, Atmos Chem Phys, 10(10), 4909–4929, doi:10.5194/acp-10-4909-2010, 2010a.

Russo, R. S., Zhou, Y., Haase, K. B., Wingenter, O. W., Frinak, E. K., Mao, H., Talbot, R. W. and Sive, B. C.: Temporal variability, sources, and sinks of C1-C5 alkyl nitrates in coastal New England, Atmos Chem Phys, 10(4), 1865–1883, doi:10.5194/acp-10-1865-2010, 2010b.

Simpson, I. J., Blake, N. J., Blake, D. R., Atlas, E., Flocke, F., Crawford, J. H., Fuelberg, H. E., Kiley, C. M., Meinardi, S. and Rowland, F. S.: Photochemical production and evolution of selected C2–C5 alkyl nitrates in tropospheric air influenced by Asian outflow, J. Geophys. Res. Atmospheres, 108(D20), 8808, doi:10.1029/2002JD002830, 2003.

Simpson, I. J., Andersen, M. P. S., Meinardi, S., Bruhwiler, L., Blake, N. J., Helmig, D., Rowland, F. S. and Blake, D. R.: Long-term decline of global atmospheric ethane concentrations and implications for methane, Nature, 488(7412), 490–494, doi:10.1038/nature11342, 2012.

Sive, B. C.: Atmospheric Nonmethane Hydrocarbons: Analytical Methods and Estimated Hydroxyl
5   Radical Concentrations, University of California, Irvine., 1998.

Sive, B. C., Zhou, Y., Troop, D., Wang, Y., Little, W. C., Wingenter, O. W., Russo, R. S., Varner, R. K. and Talbot, R.: Development of a Cryogen-Free Concentration System for Measurements of Volatile Organic Compounds, Anal. Chem., 77(21), 6989–6998, doi:10.1021/ac0506231, 2005.

Stein, A. F., Draxler, R. R., Rolph, G. D., Stunder, B. J. B., Cohen, M. D. and Ngan, F.: NOAA's
10   HYSPLIT Atmospheric Transport and Dispersion Modeling System, Bull. Am. Meteorol. Soc., 96(12), 2059–2077, doi:10.1175/BAMS-D-14-00110.1, 2015.

Strode, S. A., Rodriguez, J. M., Logan, J. A., Cooper, O. R., Witte, J. C., Lamsal, L. N., Damon, M., Van Aartsen, B., Steenrod, S. D. and Strahan, S. E.: Trends and variability in surface ozone over the United States, J. Geophys. Res. Atmospheres, 120(17), 2014JD022784, doi:10.1002/2014JD022784,
15   2015.

Sullivan, J. T., McGee, T. J., Langford, A. O., Alvarez, R. J., Senff, C. J., Reddy, P. J., Thompson, A. M., Twigg, L. W., Sumnicht, G. K., Lee, P., Weinheimer, A., Knote, C., Long, R. W. and Hoff, R. M.: Quantifying the contribution of thermally driven recirculation to a high-ozone event along the Colorado Front Range using lidar, J. Geophys. Res. Atmospheres, 2016JD025229, doi:10.1002/2016JD025229,
20   2016.

Sun, H., Trabue, S. L., Scoggin, K., Jackson, W. A., Pan, Y., Zhao, Y., Malkina, I. L., Koziel, J. A. and Mitloehner, F. M.: Alcohol, Volatile Fatty Acid, Phenol, and Methane Emissions from Dairy Cows and Fresh Manure, J. Environ. Qual., 37(2), 615–622, doi:10.2134/jeq2007.0357, 2008.

Swarthout, R. F., Russo, R. S., Zhou, Y., Hart, A. H. and Sive, B. C.: Volatile organic compound
25   distributions during the NACHTT campaign at the Boulder Atmospheric Observatory: Influence of urban and natural gas sources, J. Geophys. Res. Atmospheres, 118(18), 10,614-10,637, doi:10.1002/jgrd.50722, 2013.

Swarthout, R. F., Russo, R. S., Zhou, Y., Miller, B. M., Mitchell, B., Horsman, E., Lipsky, E., McCabe, D. C., Baum, E. and Sive, B. C.: Impact of Marcellus Shale Natural Gas Development in Southwest
30   Pennsylvania on Volatile Organic Compound Emissions and Regional Air Quality, Environ. Sci. Technol., 49(5), 3175–3184, doi:10.1021/es504315f, 2015.

Toth, J. and Johnson, R.: Summer Surface Flow Characteristics Over Northeast Colorado, Mon. Weather Rev., 113(9), 1458–1469, doi:10.1175/1520-0493(1985)113<1458:SSFCON>2.0.CO;2, 1985.

Tzompa-Sosa, Z. A., Mahieu, E., Franco, B., Keller, C. A., Turner, A. J., Helmig, D., Fried, A., Richter, D., Weibring, P., Walega, J., Yacovitch, T. I., Herndon, S. C., Blake, D. R., Hase, F., Hannigan, J. W., Conway, S., Strong, K., Schneider, M. and Fischer, E. V.: Revisiting global fossil fuel and biofuel emissions of ethane, J. Geophys. Res. Atmospheres, 122(4), 2016JD025767, doi:10.1002/2016JD025767, 2017.

US EPA: National Emissions Inventory (NEI), [online] Available from: https://www.epa.gov/air-emissions-inventories/national-emissions-inventory-nei (Accessed 22 February 2017), 2017.

Warneke, C., Geiger, F., Edwards, P. M., Dube, W., Pétron, G., Kofler, J., Zahn, A., Brown, S. S., Graus, M., Gilman, J. B., Lerner, B. M., Peischl, J., Ryerson, T. B., de Gouw, J. A. and Roberts, J. M.: Volatile organic compound emissions from the oil and natural gas industry in the Uintah Basin, Utah: oil and gas well pad emissions compared to ambient air composition, Atmos Chem Phys, 14(20), 10977–10988, doi:10.5194/acp-14-10977-2014, 2014.

Wooldridge, G., Zeller, K. and Musselman, R.: Ozone concentration characteristics at a high-elevation forest site, Theor. Appl. Climatol., 56(3–4), 153–164, doi:10.1007/BF00866424, 1997.

Zaragoza, J., Callahan, S., McDuffie, E. E., Kirkland, J., Brophy, P., Durrett, L., Farmer, D. K., Zhou, Y., Sive, B., Flocke, F., Pfister, G., Knote, C., Tevlin, A., Murphy, J. and Fischer, E. V.: Observations of acyl peroxy nitrates during the Front Range Air Pollution and Photochemistry Éxperiment (FRAPPÉ), J. Geophys. Res. Atmospheres, 2017JD027337, doi:10.1002/2017JD027337, 2017.

Zhou, Y., Mao, H. and Sive, B. C.: Impacts of Oil and Gas Emissions on Long-term Trends in Surface Ozone in the Intermountain West National Parks During 2005 – 2015, in prep, in prep.

Zhou, Y., Shively, D., Mao, H., Russo, R. S., Pape, B., Mower, R. N., Talbot, R. and Sive, B. C.: Air Toxic Emissions from Snowmobiles in Yellowstone National Park, Environ. Sci. Technol., 44(1), 222–228, doi:10.1021/es9018578, 2010.
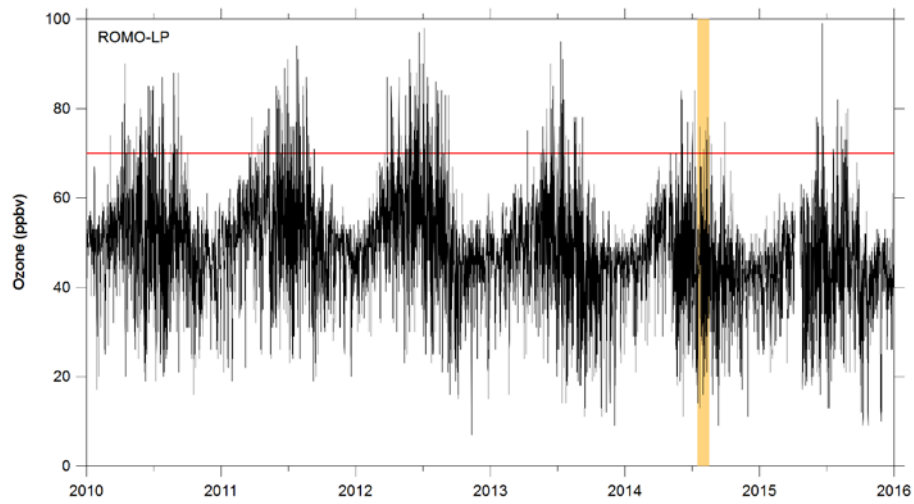
5

Figure 1. Hourly O$_3$ measurements at ROMO-LP from January 2010 to December 2015. The red line indicates the current NAAQS 8-hr daily maximum value of 70 ppb. The shaded region designates the FRAPPÉ study period.
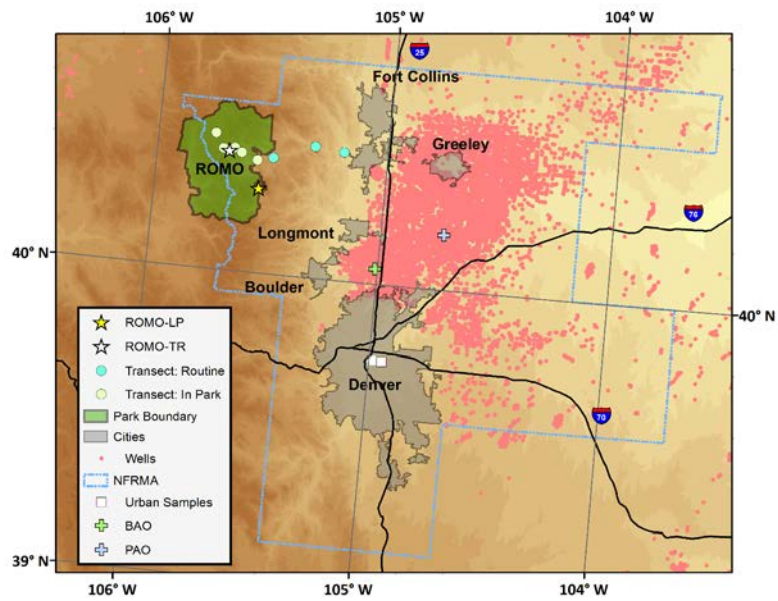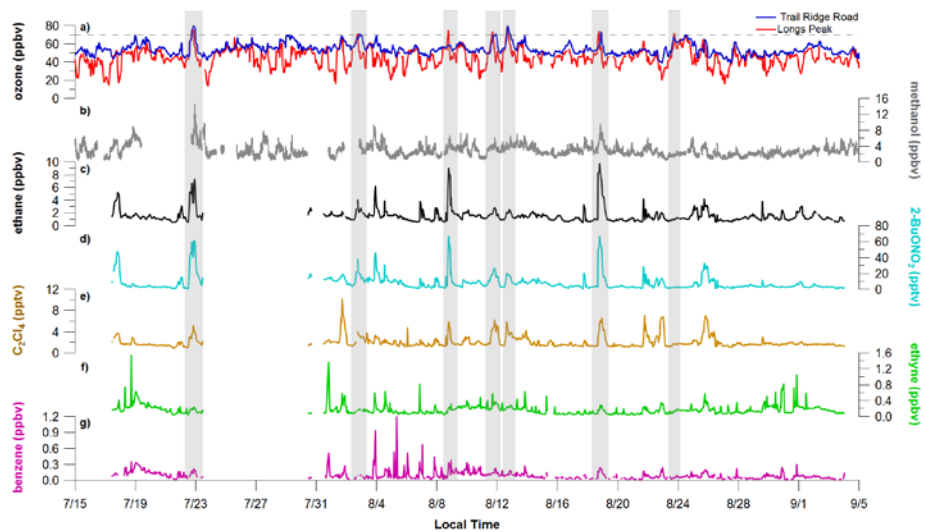
Figure 2. Map of sampling sites, including locations of the transect samples. Also shown are oil and gas well locations (COGCC, 2018) and cities along the NFRMA.

5

Figure 3. A subset of VOCs measured at the ROMO-LP site from 17 July to 4 September 2014. From 19-22 and 23-30 July, the PTR-MS and GC system, respectively, were shut down due to air conditioner failures in the field laboratories. Ozone measurements from both the ROMO-LP (Longs Peak) and ROMO-TR (Trail Ridge Road) sites are also shown. Shaded areas represent periods selected for further analysis when hourly O_3 exceeded 70 ppb (dashed line).
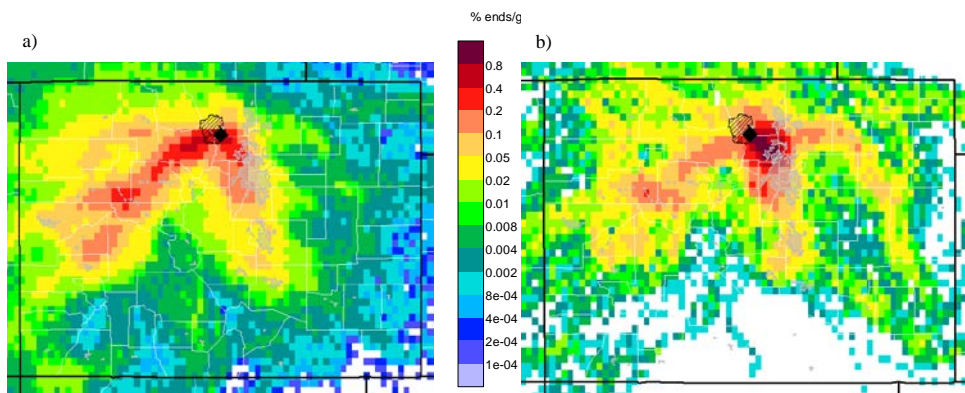
Figure 4. Residence time maps showing areas up to 2 days upwind of ROMO-LP (black diamond) during (a) all hours of the study period (July 17 – Sept 4, 2014) and (b) during hours with ethane > 90th percentile. Colours indicate the relative frequency of transport. Light grey overlay indicated urban areas. <u>Units are the percent of total endpoints in each grid cell. Endpoints are upwind air mass locations calculated every hour for two days back in time for every trajectory that arrived at the receptor during the duration of the study period.</u>
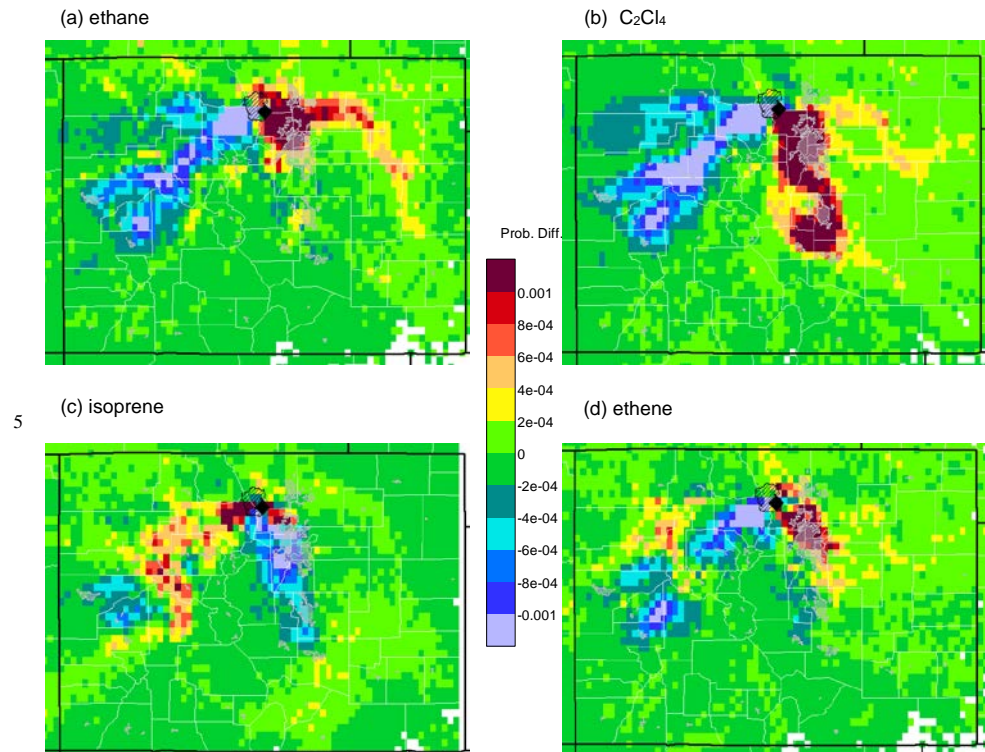
(a) ethane

(b) C₂Cl₄

(c) isoprene

(d) ethene

Prob. Diff.

Figure 5. Differences between upwind transport during hours of 90ᵗʰ percentile or higher mixing ratios and average conditions during the study (HRT-ORT) for (a) ethane, (b) C₂Cl₄, (c) isoprene, and (d) ethene. Yellow to red colours indicate areas that were more likely than average to be upwind during the 2 days prior to a high concentration measurement at ROMO-LP (black diamond). Blue to purple colours indicate areas that were less likely to be upwind, while areas in green had similar likelihoods of being upwind during average hours and during high mixing ratio hours. Light grey overlay indicated urban areas.
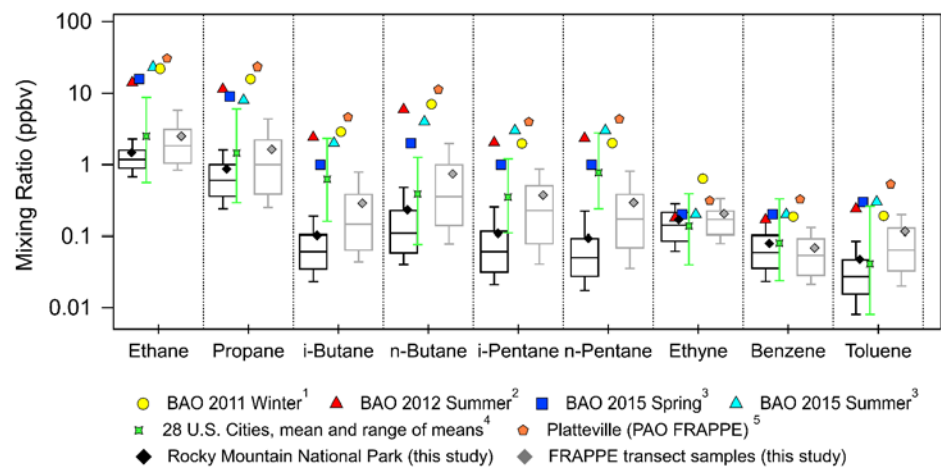
Figure 6. Box plots for mixing ratios of selected VOCs in ROMO hourly samples (black) and all transect canister samples (grey) and mean mixing ratios from previous studies ([1]Swarthout et al. (2013), [2]McDuffie et al. (2016) [3]Abeleria et al. (2017), [4] Baker et al. (2008), [5] Halliday et al. (2016)). Median mixing ratios from this study are shown as the black horizontal lines, the means are shown as the diamond symbols, the top and bottom of the boxes are the 75th and 25th percentiles and the whiskers are the 90th and 10th percentiles. The error bars on the Baker et al. (2008) data represent the maximum and minimum means observed across the cities. The data from Swarthout et al. (2013) are a mean of hourly canisters collected from noon on Feb 18, 2011- noon March 13, 2011. The McDuffie et al. (2016) data are a mean of in situ measurements made every 25 min from July 27 2012-August 12 2012. Abeleria et al. (2017) collected in situ hourly data and the values shown are means. PAO canisters were typically collected 2-3 times a day most days from 7/17-8/10, the data can be found in NASA Langley's data repository (https://www-air.larc.nasa.gov/data.htm).
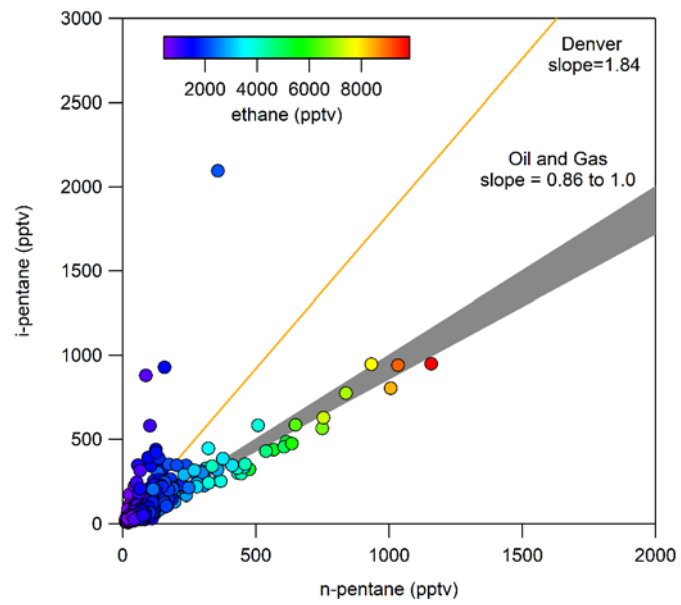
5

Figure 7. Iso-pentane versus n-pentane for ROMO hourly samples, coloured by ethane mixing ratio. For reference, also shown are the i- to n-pentane ratio for measurements collected in Denver (Baker et al., 2008) and a range of slopes from 0.86 to 1 line where everything that falls in this range indicates oil and gas influenced (COGCC, 2007; Gilman et al., 2013).
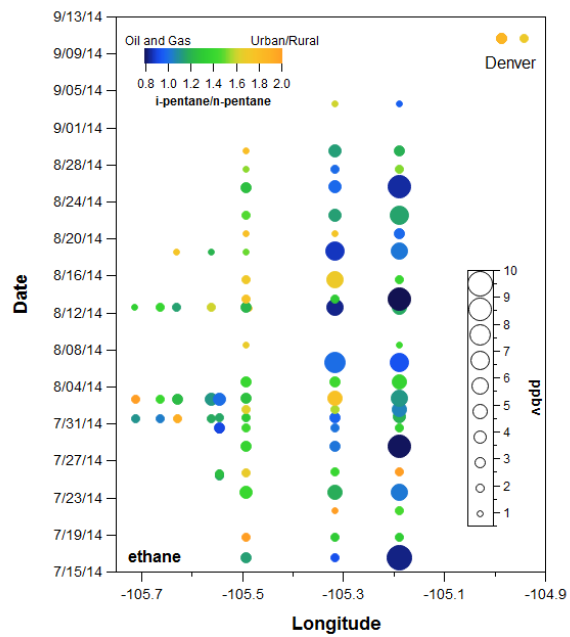
Figure 8. VOC canister data plotted by longitude and date with ethane mixing ratio represented by the size of each point and the i- to n-pentane represented by the colour. Locations correspond to transect samples shown in Figure 2.
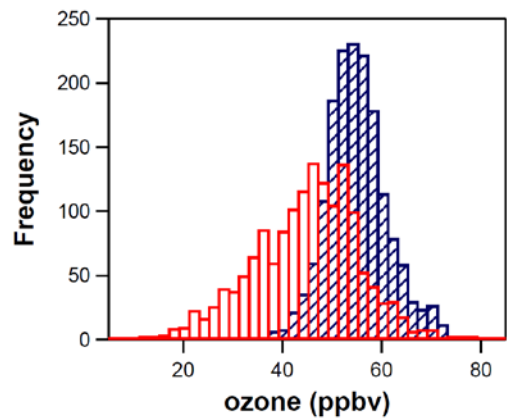
5

Figure 9. Distribution of the O₃ mixing ratios at the ROMO-LP (red) and ROMO-TR (blue) sites for the entire study period.

5
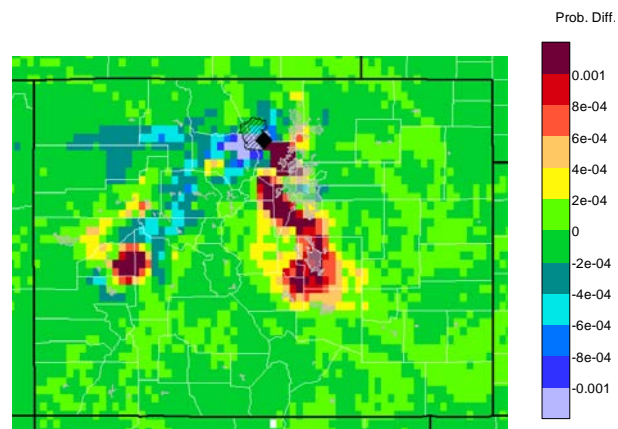
Figure 10. Differences between upwind transport during hours of 90th percentile or higher mixing ratios and average conditions during the study (HRT-ORT) for O₃. Warm colours indicate areas that were more likely than average to be upwind during the 2 days prior to a high mixing ratio measurement at ROMO-LP. Cool colours indicate areas that were less likely to be upwind, while areas in green had similar likelihoods of being upwind during average and high mixing ratio hours.

10

Oil & Gas

Aug 8 & Aug 18

i/n-pentane <1

Total ~~NVOCMHC~~-OHR=1.26 s^{-1}

Alkanes 40%
Alkenes 12%
Ethyne 0.4%
Isoprene 7%
Aromatics 1.6%
OVOCs 39%

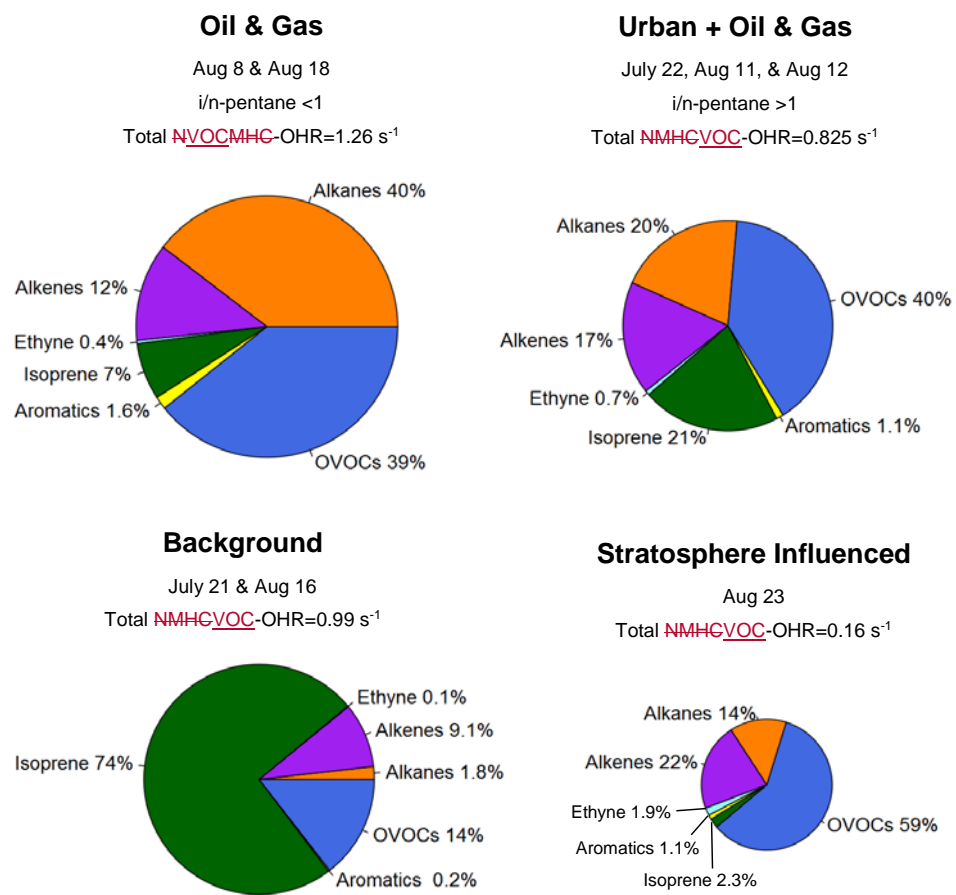**Urban + Oil & Gas**

July 22, Aug 11, & Aug 12

i/n-pentane >1

Total ~~NMHC~~VOC-OHR=0.825 s^{-1}

Alkanes 20%
OVOCs 40%
Alkenes 17%
Ethyne 0.7%
Isoprene 21%
Aromatics 1.1%

Background

July 21 & Aug 16

Total ~~NMHC~~VOC-OHR=0.99 s^{-1}

Ethyne 0.1%
Alkenes 9.1%
Isoprene 74%
Alkanes 1.8%
OVOCs 14%
Aromatics 0.2%

Stratosphere Influenced

Aug 23

Total ~~NMHC~~VOC-OHR=0.16 s^{-1}

Alkanes 14%
Alkenes 22%
Ethyne 1.9%
Aromatics 1.1%
Isoprene 2.3%
OVOCs 59%

Figure 11. Contributions to •OH reactivity (OHR) for the high O$_3$ days for peak O$_3$ hours as shown in Table 2. Days with high O$_3$ were grouped by the ratio of i- to n-pentane for oil and gas influenced and urban influenced air masses. Background days, defined by the lowest 10th percentile for ethane, and the stratospheric influenced period are used for comparison to the high O$_3$ days resulting from anthropogenic activities. The size of each pie chart is proportional to the total OHR for the given type of air mass. Reactivity was calculated using rate constants from Atkinson and Avery (2003) and Atkinson (1986).
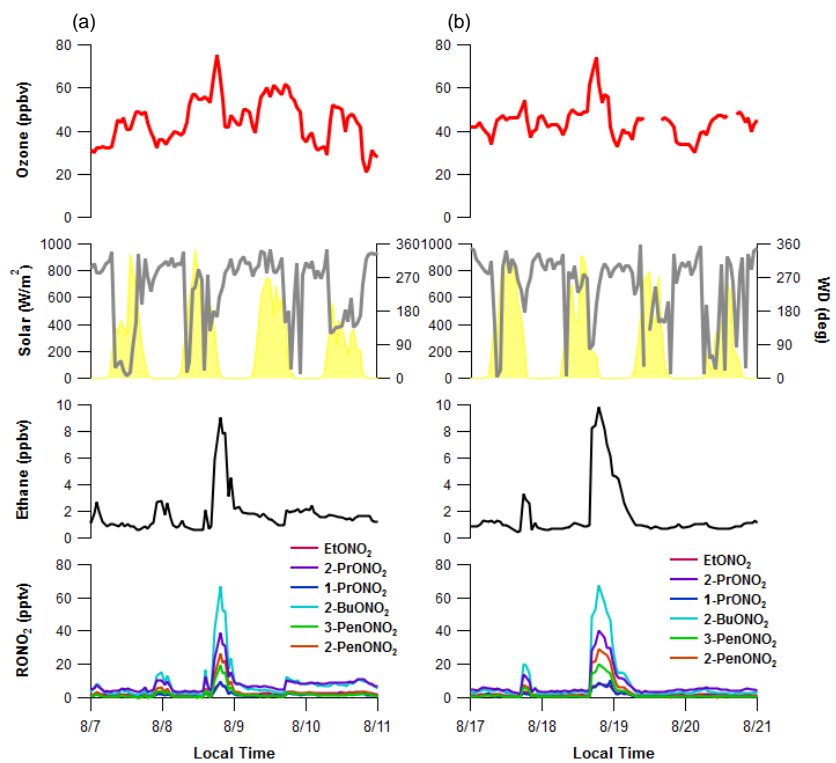
Figure 12. Time series plots of O_3, solar radiation, wind direction, ethane, and the C_2-C_5 alkyl nitrates during the a) August 8 and b) August 18 upslope events.
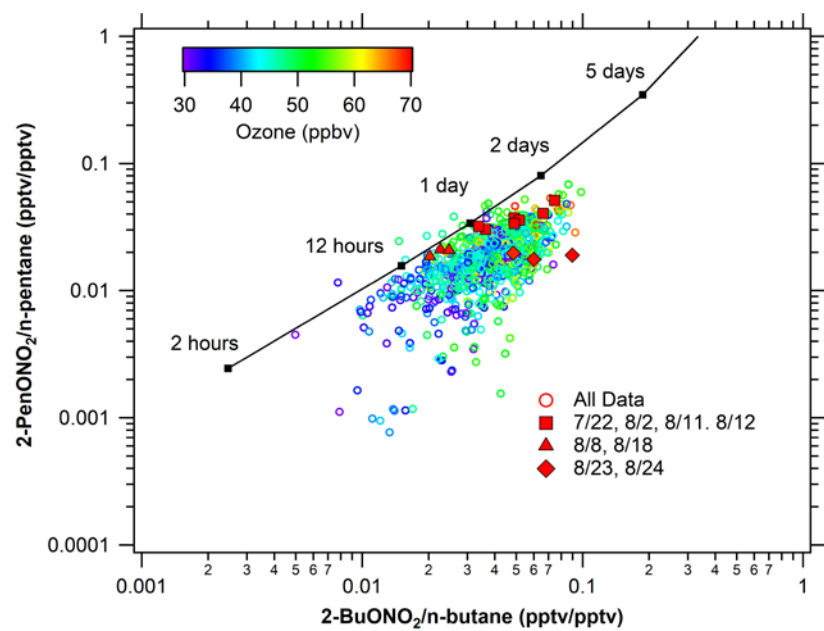
Figure 13. Photochemical age of alkyl nitrates. Comparison of observed alkyl nitrate: parent hydrocarbon ratios to predicated values provide an estimate of photochemical age.
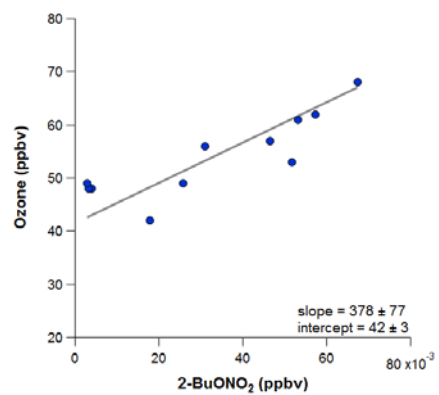
5

Figure 14. The orthogonal distance linear relationship of O₃ with 2-butyl nitrate during the August 18 event, when the park was clearly influenced by an air mass containing oil and gas emissions. This relationship is used in estimating the excess O₃ produced due to oil and gas emissions.
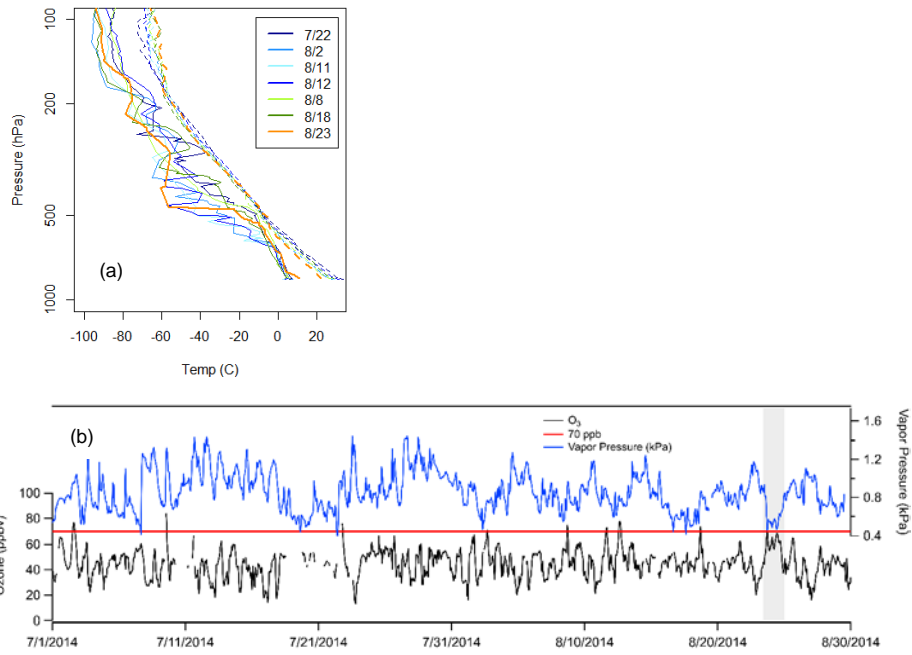
Figure 15. a) Denver soundings (http://weather.uwyo.edu/upperair/sounding.html) from high O₃ days, showing surface temperature
(dashed lines) and dew point (solid lines). **b)** Measured O₃ concentration and water vapour at ROMO-LP during the study period.
The event from August 23 is highlighted with grey shading.

Table 1. VOCs measured using the *in situ* GC system and PTR-MS at ROMO-LP. Also denoted are gases reported from the transect canister samples. Statistics are given for the GC and select PTR-MS data.

5

		Average	Median	Max.	Min.	Standard Deviation	Measured in Canister Samples?
		Mixing Ratio (ppt)					
ethane	GC	1516	1255	9800	485.0	1061	x
propane	GC	872.0	616	6842	65.2	991	x
i-butane	GC	103.0	61.3	1158	11.1	141.0	x
n-butane	GC	233.0	110.0	2978	18.8	374.0	x
ethyne	GC	168.7	141.4	1547	17.3	129.4	x
i-pentane	GC	144.0	61.9	2095	7.3	168.0	x
n-pentane	GC	97.5	50.7	1712	8.7	151.0	x
cyclopentane	GC	7.5	4.9	148.0	0.6	9.7	
n-hexane	GC	34.0	16.0	1113	1.8	70.6	x
n-heptane	GC	15.6	8.7	396.0	0.5	29.4	x
n-octane	GC	13.4	6.4	304.0	1.0	26.4	
n-nonane	GC	10.6	5.7	151.0	1.1	17.7	x
ethene	GC	113.0	87.0	1497	26.3	111.0	
propene	GC	712.0	72.9	762.0	3.6	53.4	
t-2-butene	GC	4.7	3.2	80.6	1.0	5.7	
1-butene	GC	6.5	5.2	84.8	1.1	6.0	
i-butene	GC	14.7	12.6	74.0	1.7	8.5	
c-2-butene	GC	5.6	3.4	76.3	1.0	7.1	
isoprene	GC	113.6	55.1	1559	1.0	185.5	x
a-pinene	GC	68.6	25.8	602.7	1.0	98.2	x
b-pinene	GC	84.4	39.7	821.3	1.0	110.4	x
toluene	GC	48.8	27.4	820.0	2.3	76.5	x
ethylbenzene	GC	17.6	7.5	128.0	1.1	26.6	x

m+p-xylene	GC	50.9	11.8	471.0	2.0	92.9	x
o-xylene	GC	20.2	5.5	168.0	1.3	32.2	x
C_2HCl_3	GC	0.7	0.5	3.0	0.1	0.6	x
C_2Cl_4	GC	2.0	1.6	10.2	0.9	1.1	x
CH_3I	GC	0.5	0.5	1.8	0.0	0.3	
CH_2Br_2	GC	0.8	0.8	1.1	0.5	0.1	
$CHBrCl_2$	GC	0.8	0.7	1.6	0.4	0.2	
$CHBr_3$	GC	0.6	0.6	1.6	0.1	0.2	
$MeONO_2$	GC	6.0	5.9	11.7	3.2	1.2	x
$EtONO_2$	GC	2.7	2.4	11.8	1.1	1.4	x
$i\text{-}PrONO_2$	GC	7.6	5.7	39.0	1.8	5.5	x
$n\text{-}PrONO_2$	GC	1.8	1.3	10.1	0.4	1.3	x
$2\text{-}BuONO_2$	GC	7.8	4.4	67.5	0.8	9.2	x
$3\text{-}PenONO_2$	GC	1.9	0.9	19.9	0.1	2.6	x
$2\text{-}PenONO_2$	GC	2.4	1.2	29.2	0.1	3.7	x
methanol	PTRMS	2780	2510	11400	660	1330	
acetaldehyde	PTRMS	380	320	2220	60	250	
acetone	PTRMS	1270	1100	3790	120	670	x
acetic acid	PTRMS	1060	1010	3800	50	540	
MVK+MACR	PTRMS	137	122	414	25	65	
MEK	PTRMS	130	100	670	20	91	
monoterpenes	PTRMS	160	130	680	50	92	
benzene	PTRMS	85	76	370	30	35	x
toluene	PTRMS	63	53	560	20	39	
C_8 aromatics	PTRMS	120	110	770	40	60	
C_9 aromatics	PTRMS	110	100	340	80	50	

Table 2. Summary of high O$_3$ events where at least 1 hour exceeded 70 ppb. Timing of the exceedance and the average peak concentration for both the Longs Peak and Trail Ridge monitoring sites are also included. Times shown are local.

	ROMO-LP			ROMO-TR	
	hours exceeding 70 ppb	average for exceedance	i- to n-pentane	hours exceeding 70 ppb	average for exceedance
7/22/2014	17:00-20:00	74	1.12	17:00-22:00	77
8/2/2014	17:00	71	1.05	20:00-21:00	71
8/8/2014	17:00	75	0.97	–	–
8/11/2014	15:00-16:00	73	1.44	17:00, 20:00, 21:00	70
8/12/2014	14:00-17:00	76	1.32	15:00-20:00	74
8/18/2014	17:00	74	0.97	20:00-21:00	72
8/23/2014	17:00	72	1.36	–	–
8/24/2014	–	–	–	11:00	70

5

Table 3. Summary of the O₃/RONO₂ slopes (ppbv/ppbv), intercept values (ppbv), the range of O₃ attributable to each parent alkane, and the average O₃ attributable to each parent alkane based on the correlation in each of the O₃-alkyl nitrate scatter plots for the upslope events on August 8 and August 18. An orthogonal distance regression was used to determine the slope and intercept.

5

	RONO₂	Slope (O₃/RONO₂)	Intercept (ppbv)	Attributed O₃ Range Min–Max (ppbv)	Attributed O₃ Range Ave (ppbv)
August 8 Event	EtONO2	2.9E+03	42	20 – 26	22
16:00-18:00	i-PrONO2	7.9E+02	40	24 – 30	27
(MST)	n-PrONO2	2.6E+03	44	17 – 24	20
	2-BuONO2	4.2E+02	43	22 – 28	24
	3-PenONO2	1.1E+03	46	16 – 21	18
	2-PenONO2	8.7E+02	45	18 – 23	20
August 18 Event	EtONO2	2.7E+03	41	18 – 23	20
15:00-18:00	i-PrONO2	6.3E+02	41	19 – 25	21
(MST)	n-PrONO2	2.1E+03	44	13 – 21	16
	2-BuONO2	3.8E+02	42	18 – 26	21
	3-PenONO2	1.0E+03	45	14 – 20	17
	2-PenONO2	7.3E+02	45	16 – 21	18

Table 4. Percentage contributions of the light alkanes to the alkane OHR during the oil and gas influenced events at ROMO during FRAPPÉ (Total alkane OHR =0.62 s⁻¹) and from measurements at the BAO and PAO (¹Swarthout et al. (2013), ²McDuffie et al. (2016), ³Abeleria et al. (2017), ⁴Halliday et al. (2016)).

	ROMO Summer 2014	BAO Winter 2011[1]	BAO Summer 2012[2]	BAO Spring 2015[3]	BAO Summer 2015[3]	PAO Summer 2014[4] [5]
ethane	8	8	6	11	10	7
propane	26	27	22	30	19	22
i-butane	9	9	9	6	7	9
n-butane	24	25	24	15	19	23
i-pentane	13	11	14	15	19	13
n-pentane	13	12	16	15	19	15
C_6-C_9	8	7	10	8	7	11
$\sum OHR_{alkane}$ (s⁻¹)	0.61	1.59	1.52	0.66	1.04	3.07